Neuron Scale Modeling of Prion Production with the Unfolded Protein Response

Mostafa Adimy, Louis Babin, Laurent Pujo-Menjouet

Neuron scale modeling of prion production with the Unfolded Protein Response*

January 30, 2023

Mostafa Adimy[1,2], Louis Babin[1,2], Laurent Pujo-Menjouet[1,2,3]
[1]Univ Lyon, Université Claude Bernard Lyon 1, CNRS UMR 5208, Inria,
[2]Institut Camille Jordan, F-69603 Villeurbanne, France,
Inria Lyon, Bâtiment CEI-2, 56, Boulevard Niels Bohr, F-69603 Villeurbanne, France,
[3] corresponding author
e-mail: mostafa.adimy@inria.fr, louis.babin@etu.univ-lyon1.fr, pujo@math.univ-lyon1.fr

Abstract

We develop a mathematical model that describes concentration dynamics of PrP^C and PrP^{Sc} prion proteins at the neuron scale and includes the effect of the Unfolded Protein Response (UPR). We first introduce a single neuron model taking the UPR mechanism into account. We investigate it and propose a stability study among which a bifurcation analysis with respect to three of its parameters. Then, we generalize it to two neurons showing PrP^{Sc} proteins interaction. Stability results are given when neurons exhibit identical parameters but interact differently (strong, weak or no interaction).

Keywords: Prion, Unfolded Protein Response, Delay Differential Equation, Hopf bifurcation, prion Modeling, Neurodegenerative Model
AMS: 34K18, 34K20, 37G99, 37N25, 92B05, 92C20

1 Introduction

Prions are proteins capable of existing in multiple shapes (or conformations). The normal form, denoted PrP^c (for Prion Protein Cellular), is a cell surface protein mainly expressed by neurons [32]. However, PrP^c can change its conformation to become a misfolded PrP^{Sc} (for Prion Proteins Scrapie) pathological element for mammals. They are responsible for the so called prion-diseases, also known as Transmissible Spongiform Encephalopathies, among which one can include the Creutzfeldt-Jakob disease in humans or the Bovine Spongiform Encephalopathy in cattle [29, 32]. In prion diseases, an initial seed of PrP^{Sc}, either inherited, infectious (acquired) or sporadic (spontaneous) [28], converts

*Submitted to the editors /09/21.

PrP^C and produces *de novo* PrP^{Sc} that aggregate extra-cellularly and spread the process. In fact, PrP^{Sc} become templating interfaces, inducing the misfolding of PrP^c. This mechanism is known as propagated protein misfolding [44]. It is thought to be at stake in the pathogenesis of prion-diseases but also of a larger group of neuro-degenerative disorders commonly labeled as Protein Misfolding Disorders (PMDs) including Parkinson's or Alzheimer's diseases [18, 16].

Actually PMDs share a common hallmark: some specific proteins[1] misfold, aggregate, replicate and propagate in a prion-like mechanism [18, 40, 41]. In this paradigm, pathogenic proteins, generally assembled in oligomers or aggregates, act as corruptive templates that trigger the misfolding of otherwise normally folded proteins [28, 41, 44].

The Unfolded Protein Response (UPR) is another biological phenomenon that seems to be involved in PMDs [18, 20, 21, 16, 39]. UPR is a cellular mechanism that aims to recover protein homeostasis in a reaction to Endoplasmic Reticulum (ER) stress [39, 20]. The link between misfolded proteins involved in PMDs, ER stress and UPR is still not clear : underlying mechanisms and consequences are the subject of current research (for review see *e.g.* [18, 39, 20, 21]). Nonetheless, studies seem to agree on the fact that accumulation[2] of abnormally folded proteins triggers ER stress that subsequently activate the UPR [27, 39, 20, 38, 33].

In the context of prion-diseases, knowledge becomes clearer as some studies performed on mice highlight links between PrP^{Sc} aggregates, ER stress and UPR mechanism [19, 45, 27, 26, 43, 38, 33]. For instance, some works seem to indicate that UPR downregulates PrP^{Sc} through secreted chaperones acting over the extracellular proteostasis [15, 16]. Other studies, investigating the role of UPR upon neurodegeneration in prion diseases, indicate that a high concentration of PrP^{Sc} triggers ER stress. This activates the UPR and results in a transient global shutdown of protein synthesis [27, 26, 43, 38, 33]. The latter studies, which will constitute the basis of our biological assumptions, lead us to suggest that UPR indirectly downregulates PrP^{Sc} : by preventing global protein translation, UPR activation shuts down the production of PrP^c which ultimately hampers the production of PrP^{Sc}.

It appears that, as the influence and effects of UPR on prion diseases are still unclear, mathematical models may provide valuable insights. Actually, they have already been used to investigate different issues in prion diseases and PMDs (for reviews see [36, 10]). They focus on some aspects of the disease such as the propagated misfolding mechanism and the aggregate size distribution [24, 31, 17, 13, 30, 9, 8, 11], the spatio-temporal progression of misfolded proteins (see *e.g* [1, 6, 7, 48, 4, 3] in Alzheimer's disease or [42, 25] in prion-diseases) or the strain diversity of prions [23]. However, to the best of our knowledge, there is no existing model describing PrP^{Sc} production in the framework of neuronal UPR.

The few existing mathematical approaches of UPR lie in the framework of gene regulatory networks and focus neither on neurons nor on prion proteins. They deal with the concentration dynamics of unfolded and/or misfolded proteins through different biological pathways of UPR [34, 12, 49, 47, 46]. Closer to our work here, Trusina *et al.* [47, 46] developed a model describing regula-

[1] characteristic of the disease : amyloid-beta and tau in Alzheimer's disease, α-synuclein in Parkinson's disease and prion proteins in Prion-related diseases

[2] intra or extra cellularly depending on the disease

tion of unfolded proteins inside the cell when submitted to a manageable[3] ER stress. They incorporated the main UPR-pathways acting over unfolded proteins concentrations among which we find translation attenuation, a mechanism analogous to the translation shutdown we wish to take into account. In order to proceed to mathematical analysis and qualitative investigations, we only focus, in our study, on the latter mechanism and integrate it into a simple model of prion production.

Here, we propose a mathematical modeling that describes PrP^c and PrP^{Sc} concentrations at the neuron scale and incorporates the role of UPR through an induced shutdown of global protein synthesis. Based on recent studies [27, 26, 43, 38, 33], we model the effect UPR with a negative feedback mechanism reflecting a global translation attenuation. To do so, we suppose that a high concentration of misfolded PrP^{Sc} around neurons triggers ER stress and UPR activation. This shuts down global protein translation thus reducing cellular PrP^c synthesis and as well as PrP^{Sc} production. For simplicity, we neglect the influence of UPR-induced secreted chaperones over aggregation and templating (whose effect is likely to be less important compared to global translation shutdown) and thus do not take into account the PrP^{Sc} downregulation through secreted chaperones.

Our mathematical approach is based on previous studies dedicated to delay differential equations and bifurcation analysis [22, 5, 2, 14]. In 2 we introduce our new model. We give some of its properties and study the asymptotic stability of its steady states. In 3, we extend our system to two neurons whose associated scrapie prion concentrations can interact. We finally discuss and conclude this work in 4.

2 Model of prion production at the neuron scale

Before studying a complete model with several billions of neurons, let start by investigating the process in the environment of a single cell. This section is then dedicated to the UPR acting on one neuron only.

2.1 The model

Our model, illustrated in 1, consists in describing the concentration dynamics of PrP^c and PrP^{Sc} proteins produced by a single neuron. We note x and y the concentrations of PrP^c and PrP^{Sc} respectively. They are ruled, for $t > 0$, by the following system,

$$\begin{aligned}\frac{\mathrm{d}x}{\mathrm{d}t}(t) &= KA(t) - \mu x(t) - dx(t)y(t),\\ \frac{\mathrm{d}y}{\mathrm{d}t}(t) &= dx(t)y(t) - \alpha y(t),\end{aligned}$$

where $K > 0$ represents the PrP^c production rate of the neuron and $d > 0$ characterizes the strength of the interaction between PrP^c and PrP^{Sc}. The term $dx(t)y(t)$ stands for the concentration of newly produced PrP^{Sc}. Parameter $\mu > 0$ describes the metabolic loss rate of PrP^c and $\alpha > 0$ the rate at which

[3] *i.e.* that does not induce the apoptosis of the cell

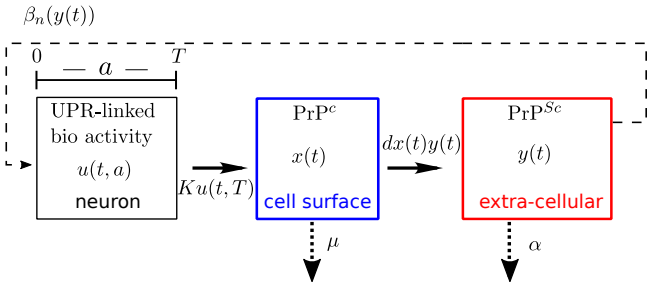

Figure 1: Neuron scale prion production model with Unfolded Protein Response (UPR) mechanism. A first compartment, structured by the biological processing time $a \in [0, T]$, describes the evolution of the neuron activity denoted by u. After a fixed time T, $u(t, T)$ mediates the PrP^c production rate K. Concentration of PrP^c proteins $x(t)$ decreases metabolically at a rate μ. PrP^c proteins are also converted into PrP^{Sc} at a rate d. PrP^{Sc} proteins are mainly lost through diffusion represented by the rate α. The feedback loop, standing for the UPR, is represented by a dashed line and depends on the PrP^{Sc} concentration $y(t)$ through a Hill function $\beta_n(\cdot)$. This is a negative feedback loop regulating the input of the neuron biological activity variable u.

PrP^{Sc} proteins are lost metabolically or through diffusion. Finally, $A(t)$ models the protein synthesis activity of the neuron at time t and is given by

$$A(t) = u(t, T),$$

where $T > 0$ is the biological processes duration. It represents the time taken by all biological processes linked with UPR to induce the global translation shutdown. We assume that $u(t, a)$ describes the biological activity of the neuron at time t and after a biological processing time $a \in [0, T]$. It is ruled by the following equation:

$$\frac{\partial u}{\partial t}(t, a) + \frac{\partial u}{\partial a}(t, a) = 0,\ t > 0,\ 0 < a < T. \tag{1}$$

Since PrP^{Sc} around the neuron downregulate PrP^c production. We model this negative feedback through a decreasing Hill function. The influence of PrP^{Sc} concentration over the neuron activity is then given by the input boundary condition of u as :

$$u(t, 0) = \frac{1}{1 + (y(t)/y_c)^n} := \beta_n\left(y(t)\right),\ \text{for all } t \geq 0,$$

where $n > 0$ is the UPR sensitivity to an overload of PrP^{Sc}. Parameter $y_c > 0$ is the threshold density of PrP^{Sc} over which the neuron (and its surrounding astrocytes) turn off global translation and thus PrP^c production.

In this framework, we use the method of characteristics to obtain the system of equations ruling our model :

$$\begin{aligned} \frac{\mathrm{d}x}{\mathrm{d}t} &= K\beta_n(y(t-T)) - \mu x(t) - dx(t)y(t), \\ \frac{\mathrm{d}y}{\mathrm{d}t} &= dx(t)y(t) - \alpha y(t), \end{aligned} \qquad \text{for } t > 0. \tag{2}$$

System 2 may be interpreted as follows: a high concentration of PrP^{Sc} proteins results, a biological time T later, in a decrease of PrP^{c} (term $K\beta(y(t-T))$) that consequently reduces the PrP^{Sc} production (term $dx(t)y(t)$). The amount of PrP^{Sc} surrounding the neuron decreases and misfolded protein homeostasis around the neuron is restored. Note that in this paradigm, we omit the notion of neuronal death and assume that the UPR is able to cope with the overload of PrP^{Sc} proteins.

The initial condition $u(0,\cdot)$ of the biological activity variable has been chosen in order to guarantee the well-posedness of system 2 (provided that initial conditions $(x_0, y_0(\cdot))$ are defined on $\mathbb{R}\times C\left([-T,0],\mathbb{R}\right)$). More precisely, we chose $u(0,a)=\beta_n\left(y_0(-a)\right)$ for all $a\in[0,T]$.

2.2 Model properties, steady states and characteristic equation

We state and prove some properties ensuring the well-posedness of our model as well as a result about existence of steady states.

For every non negative initial conditions $(x_0, y_0(\cdot)) \in \mathbb{R}\times C\left([-T,0],\mathbb{R}\right)$, system 2 admits a unique non negative solution $(x,y)\in C\left([0,+\infty),\mathbb{R}^2\right)$ such that

$$x(t)\leq \max\left\{x(0),\frac{K}{\mu}\right\} \text{ and } x(t)+y(t)\leq \max\left\{x(0)+y(0),\frac{K}{\min(\mu,\alpha)}\right\}, \text{ for all } t\geq 0. \tag{3}$$

Moreover, either there exists $\bar{t}\geq 0$ such that $x(\bar{t})\leq K/\mu$ and then $x(t)\leq K/\mu$ for all $t\geq\bar{t}$, or $\lim\limits_{t\to+\infty} x(t)=K/\mu$. Existence, uniqueness and positiveness of solutions can be proved by standard methods (*e.g.* see the theorems 3.1 and 3.4 of [37]), the rest of the proof consisting in a simple application of [2] (Proof of Proposition 3.1.) and the fact that $x(t)$ satisfies the differential inequality $x'(t)\leq K-\mu x(t)$.

Positive invariance and attractivity of $[0\,,\,K/\mu]\times\mathbb{R}_+$ results from equation 3.

Now, we focus on steady-states (x^*,y^*) of system 2 characterized by the following Proposition. The system 2 always admits a trivial equilibrium $(K/\mu,0)$. There exists a unique endemic steady state $(\alpha/d,\bar{y})$ with $\bar{y}$ satisfying 5 if and only if

$$R_0:=\frac{Kd}{\mu\alpha}>1. \tag{4}$$

If condition 4 holds, $\bar{y}$ is a continuously differentiable function of each model parameters. In particular, $\bar{y}$ is decreasing with respect to $\mu>0$ and $\alpha>0$ and increasing with respect to y_c and verifies

$$0<\bar{y}<\frac{\mu}{d}\left(R_0-1\right), \text{ with } \lim_{\alpha\to dK/\mu}\bar{y}=0 \text{ and } \lim_{\alpha\to 0}\bar{y}=+\infty.$$

Furthermore, if $\alpha=0$ then any solution (x,y) has the limit $\lim\limits_{t\to+\infty}(x(t),y(t))=(0,+\infty)$. A steady state (x^*,y^*) of system 2 satisfies :

$$\begin{aligned} K\beta_n(y^*) &= \mu x^* + dx^*y^*,\\ (dx^*-\alpha)y^* &= 0. \end{aligned}$$

We easily see that a trivial steady-state $(x^*, y^*) = (K/\mu, 0)$ always exists. An endemic steady state $(x^*, y^*) = (\bar{x}, \bar{y})$ with $\bar{x}, \bar{y} > 0$ would verify $\bar{x} = \alpha/d$ and

$$F(\bar{y}) := \frac{dK}{\mu\alpha}\beta_n(\bar{y}) = 1 + \frac{d}{\mu}\bar{y}. \tag{5}$$

Noticing that F is decreasing, $F(0) = dK/\mu\alpha = R_0$ and that $\lim_{y\to+\infty} F(y) = 0$, we obtain that the endemic steady state $(\bar{x}, \bar{y})$ exists if and only if condition 4 holds. Moreover, if $R_0 > 1$, we have

$$\frac{\mathrm{d}\bar{y}}{\mathrm{d}\mu} = \frac{1}{\frac{K}{\alpha}\beta_n'(\bar{y}) - 1}, \quad \frac{\mathrm{d}\bar{y}}{\mathrm{d}\alpha} = \frac{\frac{K}{\alpha^2}\beta_n(\bar{y})}{\frac{K}{\alpha}\beta_n'(\bar{y}) - 1}$$

and

$$\frac{\mathrm{d}\bar{y}}{\mathrm{d}y_c} = \frac{nK}{y_c\alpha}\left(\frac{\bar{y}}{y_c}\right)^n \beta_n(\bar{y})^2 \left(1 + \frac{nK}{y_c\alpha}\left(\frac{\bar{y}}{y_c}\right)^{n-1} \beta_n(\bar{y})^2\right)^{-1},$$

with

$$\beta_n'(y) = -\frac{n}{y_c}\left(\frac{y}{y_c}\right)^{n-1} \beta_n(y)^2, \text{ for all } y \in \mathbb{R}^+.$$

From these formulas and the implicit function theorem, we establish that $\bar{y}$ is a continuously differentiable function of each model parameters. Especially, it is decreasing with respect to $\mu > 0$, $\alpha > 0$ and increasing function of y_c.
Finally, assume that $\alpha = 0$. The system 2 implies that $y'(t) = dx(t)y(t) \geq 0$ from which we know that y is non-decreasing. By contradiction, assume that y is bounded and admits a positive limit. Then $\lim\limits_{t\to+\infty} y'(t) = 0$. So it implies that $\lim\limits_{t\to+\infty} x(t) = 0$. As $t \mapsto x'(t)$ is uniformly continuous on $(t_0, +\infty)$, $t_0 > 0$ large enough, we obtain that $\lim\limits_{t\to+\infty} x'(t) = 0$. Taking the limit as t goes to infinity in the first equation of 2 leads to a contradiction. We thus obtained that $\lim\limits_{t\to+\infty} y(t) = +\infty$. Now, we associate this result, the continuity and boundedness of x as well as the first equation of 2 to claim that there exists $\tilde{t} \geq 0$ such that x is non-increasing on $\left[\tilde{t}, +\infty\right)$. We conclude that x goes to 0 as t goes to infinity. The result is thus proven when $\alpha = 0$.

2.3 Asymptotic stability of steady states

We linearise system 2 about any steady state (x^*, y^*) and obtain

$$\begin{aligned}
\frac{\mathrm{d}u}{\mathrm{d}t} &= -(\mu + dy^*)u(t) - dx^*v(t) + K\beta_n'(y^*)v(t-T), \\
\frac{\mathrm{d}v}{\mathrm{d}t} &= dy^*u(t) - (\alpha - dx^*)v(t),
\end{aligned}$$

from which we deduce, the associated characteristic equation

$$\begin{vmatrix} \lambda + \mu + dy^* & dx^* - K\beta_n'(y^*)e^{-\lambda T} \\ -dy^* & \lambda + \alpha - dx^* \end{vmatrix} = 0. \tag{6}$$

In the next section, we focus on the roots of this equation to determine the local asymptotic stability of the steady state (x^*, y^*) under consideration.

2.3.1 Disease free equilibrium

Let us start with the disease free equilibrium. The endemic one follows in the next subsection. The trivial-steady state (disease free equilibrium) is locally asymptotically stable if and only if $R_0 \leq 1$. It is then destabilized through a transcritical bifurcation when $R_0 = 1$ (*i.e.* $dK = \mu\alpha$) and unstable otherwise. For the trivial steady-state, the characteristic equation 6 reads

$$(\lambda + \mu)\left(\lambda + \alpha - \frac{dK}{\mu}\right) = 0, \quad \lambda \in \mathbb{C}.$$

Thus, we have two eigenvalues $-\mu < 0$ and $\dfrac{dK}{\mu} - \alpha = \alpha\,(R_0 - 1)$, from which we can easily conclude local asymptotic stability when $R_0 < 1$ and instability when $R_0 > 1$. Now consider the case $R_0 = 1$. If we suppose that for all $t \geq 0$ $x(t) \geq K/\mu$, then from system 2 we have $x'(t) \leq 0$ and $y'(t) \geq 0$, for all $t \geq 0$. Since y is bounded and its only possible limit is 0, we get a contradiction. We conclude from Lemma 2.2 the existence of $\bar{t} \geq 0$ such that $x(t) < K/\mu$ for all $t \geq \bar{t}$. The second equation of system 2 implies that $y'(t) \leq (dK/\mu - \alpha)y(t) = 0$. We deduce that y is non-increasing with $\lim_{t\to+\infty} y(t) = 0$ and then the function $z : t \mapsto K\beta_n(y(t-T))/(\mu+dy(t))$ is non-decreasing whose limit when $t \to +\infty$ is given by K/μ. Using the first equation of 2 and the fact that z is non-decreasing, we observe that the function x can only change monotonicity when it intersects the curve of z coming from its left and by being non-increasing before this intersection and non-decreasing after. We conclude that there exists $\tilde{t} \geq \bar{t}$ such that for all $t \geq \tilde{t}$, $x(t) \leq z(t)$. Otherwise, $x(t) > z(t)$ for all $t \geq \bar{t}$. This means that the function x is non-increasing on $[\bar{t}, +\infty)$, which is absurd. Then, we have x non-decreasing on $[\tilde{t}, +\infty)$. We deduce that $\lim_{t\to+\infty} x(t) = K/\mu$. We proved that if $R_0 = 1$, the trivial steady state is globally asymptotically stable. The biological interpretation of Proposition 2.3.1 is that if the production term dK is smaller than the product of degradation term of the two prion species $\mu\alpha$, as one would expect, the trivial steady state is locally asymptotically stable otherwise it is unstable.

If $R_0 \leq 1$ then the trivial steady state $\left(\dfrac{K}{\mu}, 0\right)$ is globally asymptotically stable. The global asymptotic stability in the case $R_0 = 1$ has already been proved above. For the case $R_0 < 1$, we adapt the method used in [2] (Theorem 5.1).

Define the set G as

$$G = \left[0, \frac{K}{\mu}\right] \times \mathbb{R}_+.$$

For $(x, y) \in G$, we define the Lyapunov candidate V such that

$$V(x, y) = \frac{1}{2}y^2.$$

Note that V does not depend on x.

Let us denote $\dot{V} : G \to \mathbb{R}_+$, the Lie derivative of V along solutions of system 2. It follows that for all $(x, y) \in G$:

$$\dot{V}(x, y) = y.\frac{\mathrm{d}y}{\mathrm{d}t} = dxy^2 - \alpha y^2 = \left(\frac{d}{\alpha}x - 1\right)\alpha y^2.$$

But given that $(x, y) \in G$, we have $x \leq K/\mu$ and consequently

$$\dot{V} \leq \left(\frac{dK}{\mu\alpha} - 1\right) \alpha y^2(t) = (R_0 - 1)\, \alpha y^2(t),$$

hence $\dot{V}(x, y) \leq 0$, if $R_0 < 1$. Moreover, let us define the set $S = \left\{(x, y) \in G \,\middle|\, \dot{V}(x, y) = 0\right\}$. Let $(x, y) \in S$, then we have

$$(dx - \alpha)\, y^2 = 0,$$

but $0 \leq x \leq K/\mu$ and given that $R_0 < 1$ we also know that $K/\mu < \alpha/d$. Consequently it is necessary that $y(\cdot) = 0$. Hence $S = [0, K/\mu] \times \{0\}$. From the LaSalle's invariance theorem, we conclude that the set S is attractive in G.

Furthermore, for every solution $t \mapsto (x(t), y(t))$ of 2 lying in S, it follows that x is governed by $\frac{\mathrm{d}x}{\mathrm{d}t}(t) = K - \mu x(t)$, for all $t \geq 0$. Hence

$$x(t) = x(0)\mathrm{e}^{-\mu t} + \frac{K}{\mu}\left(1 - \mathrm{e}^{-\mu t}\right), \text{ for all } t \geq 0.$$

All in all, we obtain that every solution $t \mapsto (x(t), y(t))$ of 2 lying in S, is such that :

$$(x(t), y(t)) \underset{t \to +\infty}{\longrightarrow} \left(\frac{K}{\mu}, 0\right).$$

We conclude that every solution (x, y) of 2 reaching G (*i.e.* $x(t) \leq K/\mu$) for t large enough (such solution remains in G from 2.2) converges to $(K/\mu, 0)$. Now, let (x, y) be a solution of 2 such that $x(t) > K/\mu$ for all $t \geq 0$. Then from 2.2 we know that x converges to K/μ as t goes to infinity. Thus, we need to check that y goes to 0 at infinity in order to conclude about the global stability. In this situation, x is a strictly decreasing and continuous function such that $x(t) \underset{t \to +\infty}{\longrightarrow} K/\mu$. Hence, $\lim\limits_{t \to \infty} x'(t) = 0$ and taking the limit as $t \to +\infty$ in the first equation of system 2 we obtain :

$$1 + \frac{d}{\mu} \lim_{t \to \infty} y(t) = \lim_{t \to \infty} \beta_n(y(t - T)),$$

from which we obtain that $y(t)$ goes to 0 as $t \to +\infty$.

In conclusion, all solutions of system 2 tends to $(K/\mu, 0)$ if $R_0 \leq 1$ and we obtained the global stability of $(K/\mu, 0)$.

2.3.2 Endemic steady state

The characteristic equation of system 2 linearised about its endemic steady state $(\bar{x}, \bar{y}) = (\alpha/d, \bar{y})$, reads

$$\lambda^2 + a\lambda + b + c\mathrm{e}^{-T\lambda} = 0,\ \lambda \in \mathbb{C}, \tag{7}$$

with

$$\begin{aligned}
a &= \frac{dK}{\alpha}\beta_n(\bar{y}) = \mu + d\bar{y}, \\
b &= \alpha\left(\frac{dK}{\alpha}\beta_n(\bar{y}) - \mu\right) = \alpha(a - \mu), \\
c &= -K\beta_n'(\bar{y})\left(\frac{dK}{\alpha}\beta_n(\bar{y}) - \mu\right) = -K\beta_n'(\bar{y})(a - \mu).
\end{aligned}$$

The parameters a, b and c do not depend on the delay T. The characteristic equation 7 has been studied in details [22, 5, 14]. In this paper, we use their methods and results to establish a stability result about the endemic steady state and to perform a bifurcation analysis with respect to three parameters.

First, we notice that 0 is not a root of the characteristic equation 7, given that $a > 0$, $b > 0$ and $c > 0$. Then we state the following proposition about absolute stability that is stability independent of the delay [37] of the endemic steady steady state. If

$$b > c \text{ and } a^2 - 2b > -2\sqrt{b^2 - c^2}, \tag{8}$$

then the endemic steady state $(\alpha/d, \bar{y})$ is locally asymptotically stable for all $T \geq 0$, that is $Re(\lambda) < 0$ for every root $\lambda \in \mathbb{C}$ of equation 7 and all $T \geq 0$.

We apply directly Proposition 4.9 of [37] and Chapter 3.3 of [22].

Now, we state and prove a lemma about the local asymptotic stability of the co-existence equilibrium that legitimates the subsequent bifurcation analysis.

If

$$T = 0 \text{ or } y_c \to +\infty,$$

then the co-existence steady state $(\alpha/d, \bar{y})$ is locally asymptotically stable.

The local asymptotic stability when $T = 0$ simply results from the fact that $a, b, c > 0$.

Then, consider $\bar{y}$, a, b and c as functions of $y_c > 0$. We remind that we necessarily have $R_0 = dK/\alpha\mu > 1$ for the existence of the co-existence steady state. Given that $\bar{y}$ is bounded, we have $\lim\limits_{y_c \to +\infty} \frac{\bar{y}}{y_c} = 0$ from which follows that $\lim\limits_{y_c \to +\infty} \beta_n(\bar{y}) = 1$ and $\lim\limits_{y_c \to +\infty} a = \mu R_0 > 0$, $\lim\limits_{y_c \to +\infty} b = \alpha\mu\,(R_0 - 1) > 0$, $\lim\limits_{y_c \to +\infty} c = 0$. So, when $y_c \to +\infty$, the characteristic equation would thus read

$$\lambda^2 + \mu R_0 \lambda + \alpha\mu\,(R_0 - 1) = 0,\ \lambda \in \mathbb{C}.$$

If this equation admits some roots, given that $R_0 > 1$, they would always have negative real parts. All in all, the proposition is proven.

Given that $\alpha \mapsto (\bar{x}, \bar{y})$ is continuous and tends to $(0, +\infty)$ as $\alpha \to 0$, and $\lim\limits_{t \to +\infty} (x(t), y(t)) = (0, +\infty)$ for $\alpha = 0$, we claim that the steady state $(\bar{x}, \bar{y})$ is locally asymptotically stable for $\alpha > 0$ small enough. This was also confirmed by the numerical simulations.

Let $\psi \in \mathcal{P}$ be a varying parameter, the other parameters are assumed to be fixed. The set $\mathcal{P}$ gathers all possible values for the chosen parameter ψ.

If ψ is varied continuously, the only way for roots of 7 with positive real parts to appear is through the imaginary axis. We easily verify that roots with positive real parts cannot appear in the right half complex plane. Starting from parameters verifying 2.3.2, we vary ψ and see if a Hopf bifurcation occurs using the methods in [5, 14]. Given that $\lambda = 0$ is not a root of 7, we look for purely imaginary solutions $\lambda = i\omega(\psi)$, with $\omega(\psi) > 0$. We assume, implicitely, that ω is a continuously differentiable function of ψ. This property has to be verified *a posteriori*. Hence $\omega := \omega(\psi)$ verifies

$$\begin{aligned} \cos(T\omega) &= \frac{\omega^2 - 2b}{c}, \\ \sin(T\omega) &= \frac{a\omega}{c}. \end{aligned} \tag{9}$$

Summing the square of the right-hand sides, we obtain

$$\omega^4 - (2b - a^2)\omega^2 + b^2 - c^2 = 0, \tag{10}$$

which also reads $Q(\omega^2) = 0$, with the polynomial Q defined by

$$Q(X) = X^2 - SX + P, \tag{11}$$

with

$$S = -(a^2 - 2b) = 2b - a^2 \text{ and } P = b^2 - c^2,$$

the sum and the product of its roots. The discriminant of Q is

$$\Delta = (a^2 - 2b)^2 - 4(b^2 - c^2) = a^4 - 4ba^2 + 4c^2.$$

Let us define the sets

$$I_1 = \left\{ \psi \,\middle|\, b(\psi) < c(\psi) \text{ or } \left[2b(\psi) > a(\psi)^2 \text{ and } b(\psi) = c(\psi) \right] \right\},$$

and

$$I_2 = \left\{ \psi \,\middle|\, b(\psi) > c(\psi) \text{ and } a(\psi)^2 - 2b(\psi) \leq -2\sqrt{b(\psi)^2 - c(\psi)^2} \right\},$$

and remind that $\Delta(\psi) = a(\psi)^4 - 4b(\psi)a(\psi)^2 + 4c(\psi)^2 > 0$ for $\psi \in I_1 \cup I_2$. We emphasize that I_1 and I_2 may possibly consist in multiple sub-intervals of different lengths. The previous study of the polynomial Q enables us to state the following proposition (adapted from Lemma 1 of [14] and part 3.3 of [22]). (i) If $\psi \in I_1$, i.e.

$$b(\psi) < c(\psi) \text{ or } \left[2b(\psi) > a(\psi)^2 \text{ and } b(\psi) = c(\psi) \right], \tag{12}$$

then equation 10 has a single positive real root $\omega_+(\psi)$ such that

$$\omega_+(\psi)^2 = \frac{1}{2}\left[2b(\psi) - a(\psi)^2 + \sqrt{\Delta(\psi)} \right]. \tag{13}$$

(ii) If $\psi \in I_2$, i.e.

$$b(\psi) > c(\psi) \text{ and } a(\psi)^2 - 2b(\psi) \leq -2\sqrt{b(\psi)^2 - c(\psi)^2}, \tag{14}$$

then equation 10 has, on top of $\omega_+(\psi)$, a second positive real root $\omega_-(\psi)$ such that

$$\omega_-(\psi)^2 = \frac{1}{2}\left[2b(\psi) - a(\psi)^2 - \sqrt{\Delta(\psi)} \right]. \tag{15}$$

(iii) Otherwise, if $\psi \notin I_1$ and $\psi \notin I_2$, then there are no positive real roots of 10. Hence it follows that, if $I_1 = \emptyset$ and $I_2 = \emptyset$ then there are no positive real roots of 10, and no Hopf bifurcation can occur. Thanks to the latter proposition, we know that the set

$$I = I_1 \cup I_2,$$

actually gathers the values of ψ for which equation 10 has, at least one positive real root and for which Hopf bifurcation might occur.

It is thus valuable to find sufficient conditions (in terms of model parameters) under which the set I exists. This will enable us to clarify the conditions under

which stability switches are likely to happen. Hence, we first make a remark that renders aforementioned conditions over a, b and c clearer. Then we look for conditions in terms of model parameters under which 12 or 14 hold. Condition $b < c$ is equivalent to

$$\frac{Kd^2}{\alpha} < (\mu + d\bar{y})^2 \frac{n}{y_c} \left(\frac{\bar{y}}{y_c}\right)^{n-1}. \tag{16}$$

If parameters verify

$$\mu + dy_c < \frac{Kd}{2\alpha} < 2n\mu, \tag{17}$$

then $I_1 \neq \emptyset$ and $I_2 = \emptyset$. From simple arguments, the first condition $dK/2\alpha < 2n\mu$ implies that

$$0 < \left(\frac{\mu}{d}\right)^2 + \left(\frac{2\mu}{d} - \frac{K}{n\alpha}\right) y_c + y_c^2,$$

from which it follows that

$$\frac{Kd^2}{\alpha} < (\mu + dy_c)^2 \frac{n}{y_c}.$$

Moreover, the second condition $\mu + dy_c < dK/2\alpha$ added to simple considerations about equation 5 ensures that $\bar{y} > y_c$. All in all, if condition 17 holds, we have

$$\frac{Kd^2}{\alpha} < (\mu + dy_c)^2 \frac{n}{y_c} < (\mu + d\bar{y})^2 \frac{n}{y_c} \left(\frac{\bar{y}}{y_c}\right)^{n-1}.$$

From 2.3.2, we thus know that $b < c$ and we have $I_1 \neq \emptyset$ and $I_2 = \emptyset$. Reformulations of condition 17 lead to the following corollary.

(i) Let the varying parameter be $\alpha = \psi$. If parameters (different from α) verify

$$\mu + dy_c < 2n\mu,$$

then $I \neq \emptyset$ and

$$\left[\frac{Kd}{4n\mu}\,;\, \frac{Kd}{2(\mu + dy_c)}\right] \subset I_1 \subset I.$$

(ii) If $y_c = \psi$, and parameters (different from y_c) verify

$$\mu < \frac{Kd}{2\alpha} < 2n\mu,$$

then $I \neq \emptyset$ and

$$\left[0\,;\, \frac{K}{2\alpha} - \frac{\mu}{d}\right] \subset I_1 \subset I.$$

(iii) If $T = \psi$, and parameters verify condition 17 then $I = \mathbb{R}_+^*$ with $I_2 = \emptyset$ and $I_1 = I$.

Simple but long computations lead to these results. We only underline that *(iii)* is easily obtained by noticing that a, b and c are independent from T. In fact, variations of $\psi = T$ do not modify the values of $\bar{y}$, a, b and c.

2.3.2 does not give precise information on the changes in stability but still provides with sufficient conditions ensuring the existence of an interval I in which these stability switches could occur. In fact, 2.3.2 should not be considered in the context of the previously established stability of the endemic steady state when $\alpha \to 0$ or $y_c \to +\infty$. They should rather be considered as preliminary results for the existence of an interval on which a Hopf bifurcation with respect to the three parameters is possible. In the following, we assume that $I \neq \emptyset$ and vary ψ first starting from a value (possibly outside the interval I) where the endemic steady state is locally asymptotically stable and then through I where stability switches could occur.

We continue our bifurcation analysis and introduce, for all $\psi \in I$, the variable $\Theta_\pm(\psi) \in [0, 2\pi]$ such that:

$$\begin{aligned} \cos(\Theta_\pm(\psi)) &= \frac{\omega_\pm(\psi)^2 - b}{c}, \\ \sin(\Theta_\pm(\psi)) &= \frac{a\omega_\pm(\psi)}{c}, \end{aligned} \tag{18}$$

where the signs have to be adapted according to where ω_+ or ω_- are defined. Given that $\omega_\pm \geq 0$, we always have $\sin(\Theta_\pm(\psi)) \geq 0$. Consequently, $\Theta_\pm(\psi) \in [0, \pi]$ for all $\psi \in I$. Hence, we obtain for all $\psi \in I$:

$$\Theta_+(\psi) = \arccos\left(\frac{\omega_+(\psi)^2 - b}{c}\right), \tag{19}$$

and, for $\psi \in I_2$:

$$\Theta_-(\psi) = \arccos\left(\frac{\omega_-(\psi)^2 - b}{c}\right). \tag{20}$$

Then, we define the functions $z_\pm$ such that for all $\psi \in I$ and $k \in \mathbb{N}$

$$z_\pm(\psi, k) = T - \frac{\Theta_\pm(\psi) + 2k\pi}{\omega_\pm(\psi)},$$

where the sign has to be adapted accordingly. One could have thought to follow the work of [5] and use arctan functions to define Θ_+ and Θ_-. However, the signs involved in system 18 led us to use the arccos function instead. We get the following Theorem, adapted from Theorem 2.1 and 3.1 of [5]. Assume that the parameters (different from ψ) are fixed such that $I \neq \emptyset$. The characteristic equation 7 admits a pair of simple conjugate purely imaginary roots $\pm i\omega_+(\psi_+^*)$ in $\psi_+^* \in I$, with

$$\omega_+(\psi^*) = \sqrt{\frac{1}{2}\left[2b(\psi_+^*) - a(\psi_+^*)^2 + \sqrt{\Delta(\psi_+^*)}\right]}, \tag{21}$$

if and only if there exists $k \in \mathbb{N}$ such that $z_+(\psi_+^*, k) = 0$ with

$$z_+(\psi, k) = T - \frac{1}{\omega_+(\psi)}\left[\arccos\left(\frac{\omega_+(\psi)^2 - b}{c}\right) + 2k\pi\right] \text{ for all } (\psi, k) \in I \times \mathbb{N}. \tag{22}$$

Moreover, if $I_2 \neq \emptyset$ then the characteristic equation 7 admits a second pair of simple conjugate purely imaginary roots $\pm i\omega_-(\psi_-^*)$ in $\psi_-^* \in I_2$, with

$$\omega_-(\psi_-^*) = \sqrt{\frac{1}{2}\left[2b(\psi_-^*) - a(\psi_-^*)^2 - \sqrt{\Delta(\psi_-^*)}\right]}, \tag{23}$$

if and only if there exists $k \in \mathbb{N}$ such that $z_-(\psi_-^*, k) = 0$ with

$$z_-(\psi, k) = T - \frac{1}{\omega_-(\psi)} \left[\arccos\left(\frac{\omega_-(\psi)^2 - b}{c} \right) + 2k\pi \right] \text{ for all } (\psi, k) \in I_2 \times \mathbb{N}. \tag{24}$$

Furthermore, when a boundary value $\psi^* \in I$ exists and is reached due to a variation of ψ, its associated pair of simple conjugate purely imaginary roots cross the imaginary axis - possibly inducing a stability switch - from left to right if $\delta(\psi^*) > 0$ and from right to left if $\delta(\psi^*) < 0$ where

$$\delta(\psi^*) = \operatorname{sign}\left\{ \frac{\mathrm{d}(\mathrm{Re}\lambda)}{\mathrm{d}\psi}(\psi^*) \right\}.$$

For given parameter values under which $I \neq \emptyset$, a stability switch is possible only if there exists $k \in \mathbb{N}$ such that $z_+(\cdot, k)$ or $z_-(\cdot, k)$ vanish at least one time. When the parameter ψ varies from a value ψ_0 such that $(\alpha/d, \bar{y})$ is stable, a Hopf bifurcation must occur at the first boundary value ψ_h^* such that

$$\psi_h^* = \min\left\{ \psi^* \mid \text{there exists } k \in \mathbb{N} \text{ such that } z_+(\psi^*, k) = 0 \text{ or } z_-(\psi^*, k) = 0 \right\},$$

if the transversality condition $\frac{\mathrm{d}(\mathrm{Re}\lambda)}{\mathrm{d}\psi}(\psi_h^*) \neq 0$ holds. Explicit form of $\frac{\mathrm{d}(\mathrm{Re}\lambda)}{\mathrm{d}\psi}$ is obtained by differentiating the characteristic equation 7 following the branch of roots $\lambda(\psi)$ defined such that $\lambda(\psi^*) = \mathrm{i}\omega^*$ with $\omega^* = \omega_+(\psi^*)$ or $\omega^* = \omega_-(\psi^*)$ depending on the situation under consideration. After some computations, when $\psi^* = T^*$, one gets:

$$\frac{\mathrm{d}(\mathrm{Re}\lambda)}{\mathrm{d}T}(T^*) = \frac{(a^2 - 2b){\omega^*}^2 + 2{\omega^*}^4}{\left(-T^*{\omega^*}^2 + a + b\right)^2 + \left(2 + aT^*\right)^2 {\omega^*}^2}.$$

Inserting the expression of $\omega_\pm(T^*)$ into this expression always gives $\frac{\mathrm{d}(\mathrm{Re}\lambda)}{\mathrm{d}T}(T^*) > 0$ when $\omega^* = \omega_+(T^*)$ and $\frac{\mathrm{d}(\mathrm{Re}\lambda)}{\mathrm{d}T}(T^*) < 0$ when $\omega^* = \omega_-(T^*)$ (as noticed in [22]). It ensures us that if a purely imaginary root $\lambda(T^*)$ ($= i\omega_+(T^*)$ or $i\omega_-(T^*)$) exists, it is necessarily simple.

If $\psi^* \neq T^*$ (*e.g.* $\psi^* = \alpha^*$ or $\psi^* = {y_c}^*$), we have :

$$\begin{aligned}\frac{\mathrm{d}(\mathrm{Re}\lambda)}{\mathrm{d}\psi}(\psi^*) = &\frac{\left(-\frac{{\omega^*}^2}{c}\frac{\mathrm{d}c}{\mathrm{d}\psi}(\psi^*) + \frac{b}{c}\frac{\mathrm{d}c}{\mathrm{d}\psi}(\psi^*) - \frac{\mathrm{d}b}{\mathrm{d}\psi}(\psi^*)\right)\left(-T{\omega^*}^2 + a + Tb\right)}{\left(-T{\omega^*}^2 + a + Tb\right)^2 + \left(2 + Ta\right)^2 {\omega^*}^2} \\ &+ \frac{{\omega^*}^2(2 + Ta)\left(\frac{a}{c}\frac{\mathrm{d}c}{\mathrm{d}\psi}(\psi^*) - \frac{\mathrm{d}a}{\mathrm{d}\psi}(\psi^*)\right)}{\left(-T{\omega^*}^2 + a + Tb\right)^2 + \left(2 + Ta\right)^2 {\omega^*}^2}.\end{aligned}$$

When $\psi = T$, we use 2.3.2 and the previous remarks to obtain a more precise and concise result. Assume that model parameters different from T are fixed and such that $I \neq \emptyset$. If T is increased starting from 0, then the system undergoes a Hopf bifurcation at $T = T_h^*$ with

$$T_h^* = \frac{1}{\omega_+} \arccos\left(\frac{\omega_+^2 - b}{c} \right), \tag{25}$$

where $\omega_+ = \sqrt{\frac{1}{2}\left[2b - a^2 + \sqrt{a^4 - 4ba^2 + 4c^2}\right]}$. First, due to 2.3.2, we know that the co-existence steady state is locally asymptotically stable when $T = 0$.

Then, if $I \neq \emptyset$ then $I = \mathbb{R}^+$ (since a, b and c are independent from T). If they are defined, both $z_+(\cdot, k)$ and $z_-(\cdot, k)$ cross the horizontal axis (as increasing functions of T) and thus stability switches must occur at these crossings labeled T^*. Moreover, a Hopf bifurcation could happen at the smallest value T_h^* of these delays. This smallest delay correspond either (as z_+ and z_- are decreasing functions of $k \in \mathbb{N}$) to a zero of $z_+(\cdot, 0)$ or $z_-(\cdot, 0)$, if defined. If $I_2 = \emptyset$ then only $z_+(\cdot, 0)$ is well defined, thus T_h^* is the zero of this function and we consequently obtain the expression 25. If $I_2 \neq \emptyset$, then $z_+(\cdot, 0)$ and $z_-(\cdot, 0)$ are defined, thus T_h^* corresponds to the smallest zero of these two functions which is the zero of $z_+(\cdot, 0)$, as $\omega_+ > \omega_-$ and $\omega \mapsto \frac{1}{\omega} \arccos\left(\frac{\omega^2 - b}{c}\right)$ is decreasing on its interval of definition. All in all, regardless the situation, the first, *i.e.* the smallest, delay at which a stability switch occurs T_h^* corresponds to the zero of $T \mapsto z_+(T, 0)$ and is given by equation 25. Finally, we conclude that a Hopf bifurcation occurs at $T = T_h^*$ since the transversality condition $\frac{\mathrm{d}(\mathrm{Re}\lambda)}{\mathrm{d}T}(T_h^*) \neq 0$ is always verified.

In 2a, 2c and 2d we present stability diagrams obtained when $\psi = T$, α or y_c. These diagrams give us insights in the dynamics of the system in the parameter space. Boundaries (indicated by continuous or dashed lines) separate the parameter space into regions of different dynamics.
Notice that 2a and 2c are similar as they both display stability boundaries in the (T, α) plane.
In 2b we illustrate - through an arbitrary example of two model trajectories - the Hopf bifurcation that occurs as $\psi = T$ increased from 0: increasing the parameter T from a value where the endemic steady state is stable destabilizes it through a Hopf bifurcation when T reaches the first boundary value T^* ($\simeq 4.13$ days in our example).
2d presents stability boundaries in the (T, y_c) when $\psi = y_c$ is the varying parameter. In such situation, when T is set to a fixed value, decreasing the parameter y_c from infinity triggers a Hopf bifurcation when y_c reaches the first boundary value ${y_c}^*$.
From a biological point of view, the Hopf bifurcation study is important in the following sense. Our goal is to understand the start and stop mechanism of UPR which may possibly lead the neuron to show an oscillatory stress state. In other words, a neuron may leave and enter stress conditions periodically depending on its environment. If such a phenomenon occurs, this oscillatory behavior may propagate eventually to the other neurons, and some synchronicity could appear from this group. This last point will be the subject of a future work. We prove here that not only such an oscillatory behavior is possible, but we are also able to determine which parameters need to change to get it. From the study above, we manage to prove for instance that increasing the protein formation process duration T (which could happen for weak of damaged cells), may lead to oscillations in protein productions. We show that other parameters are involved such as the loss of diffusion term α or the threshold density y_c of PrP^{Sc} implying it stress condition.

We used the function `dde23` [35] from MATLAB© for numerical simulations. We underline that asymptotic solutions turned out to be independent from initial conditions and densities. We thus arbitrarily decided to compute each trajectories showed in 2b with an initial condition corresponding to 50% of the associated steady state specified by parameter values.

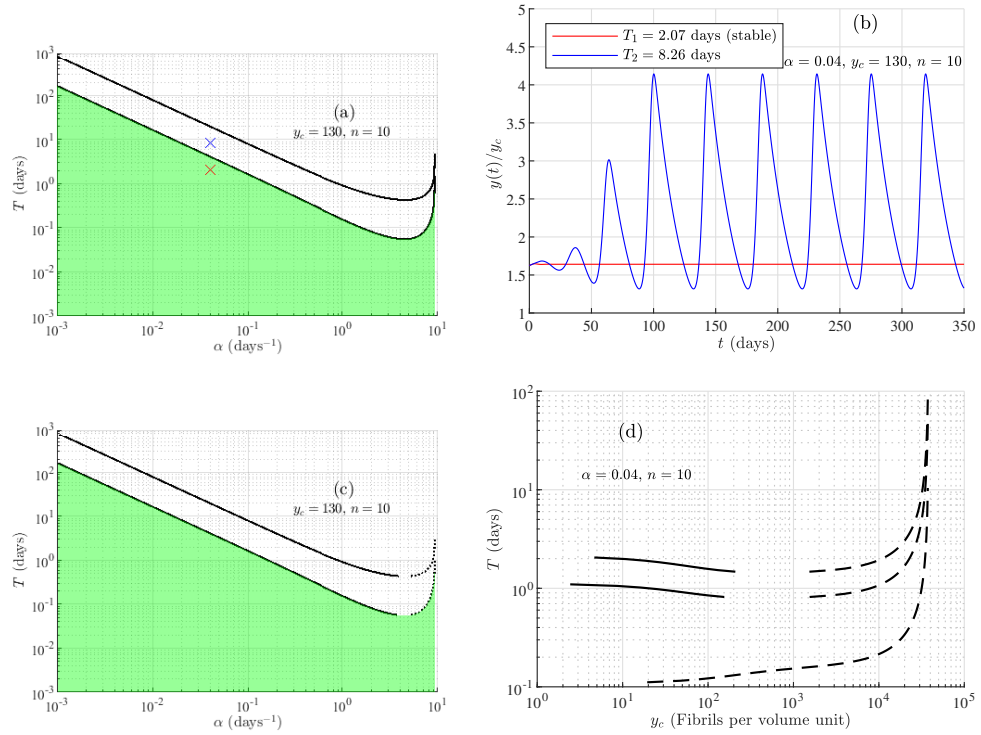

Figure 2: **(a)**, **(c)**, **(d)**: Stability diagrams in the (α, T) plane with $T = \psi$ (**(a)**) or $\alpha = \psi$ (**(c)**) as the varying parameter and in the (y_c, T) plane with $\psi = y_c$ as the varying parameter (**(d)**). Boundary parameters ($\psi^* = T^*$ in (a), $\psi^* = \alpha^*$ in (c) and $\psi^* = {y_c}^*$ in (d)) are specified by continuous ($\frac{\mathrm{d}(\mathrm{Re}\lambda)}{\mathrm{d}\psi}(\psi^*) > 0$) or dashed ($\frac{\mathrm{d}(\mathrm{Re}\lambda)}{\mathrm{d}\psi}(\psi^*) < 0$) lines. For clarity, we only plotted the two first boundaries ($k = 0$ and $k = 1$) in the (T, α) plane, the three first boundaries ($k = 1, 2, 3$) in the (T, y_c) plane and indicated in green the area where the endemic equilibrium is stable. The situation in (d) being complex, we decide not to highlight the stability area of the endemic equilibrium for clarity. The values of the parameters used to obtain these plots are specified in 1, we underline that parameter values ensure that we always have $R_0 > 1$ in each figure. **(b)**: Illustration through an arbitrary example of two trajectories before (T_1 in red) and after (T_2 in blue) the Hopf bifurcation. For all the figures, we chose the range for ψ (*i.e.* T, α or y_c) so that stability switches could appear with $I \neq \emptyset$ (*i.e.* $b(\psi) < c(\psi)$ when a stability switch occurs).

Table 1: Values of parameters used in 2. Orders of magnitude are consistent with the values used in [17, 23].

Parameters	Values	Units
T	variable	days
μ	5	days^{-1}
α	variable (2a, and 2c) or 0.04 (2b and 2d)	days^{-1}
K	1500	(Fibrils per volume unit).days^{-1}
y_c	130 (2a, 2b and 2c) or variable (2d)	Fibrils per volume unit
d	0.1	(Fibrils per volume unit)$^{-1}$.days^{-1}
n	10 (2a, 2b and 2c) or 250 (2d)	-

3 Model of prion production with 2 neurons

In this section we generalize the previous modeling and describe prion production and dynamic at the scale of two neurons. We first describe the model, then proceed to the stability analysis of the steady states.

3.1 The model

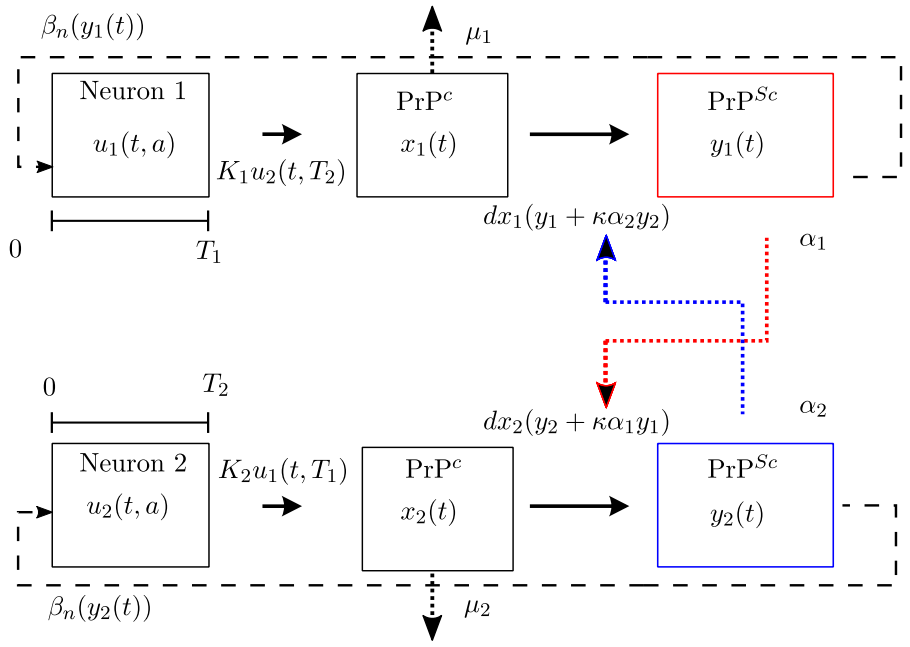

Figure 3: Two neurons' prion production model. This model generalizes the one presented in 1. Interactions between prion species are introduced through the coupling constant $\kappa \in [0,1]$ in the PrP^{Sc} production terms of the neurons: $dx_1\kappa\alpha_2x_2$ and $dx_2\kappa\alpha_1x_1$.

The model illustrated in 3 describes the dynamics of PrP^C protein concen-

trations associated to neuron 1 and neuron 2 - x_1 and x_2 - as well as the PrP^{Sc} concentrations in the close vicinity of neuron 1 and neuron 2 - y_1 and y_2. This model is governed, for $t \geq 0$, by the following system:

$$\begin{aligned}
\frac{\mathrm{d}x_1}{\mathrm{d}t} &= K_1\beta_n(y_1(t-T_1)) - \mu_1 x_1(t) - dx_1(t)\left(y_1(t) + \kappa\alpha_2 y_2(t)\right), \\
\frac{\mathrm{d}x_2}{\mathrm{d}t} &= K_2\beta_n(y_2(t-T_2)) - \mu_2 x_2(t) - dx_2(t)\left(y_2(t) + \kappa\alpha_1 y_1(t)\right), \\
\frac{\mathrm{d}y_1}{\mathrm{d}t} &= dx_1(t)\left(y_1(t) + \kappa\alpha_2 y_2(t)\right) - \alpha_1 y_1(t), \\
\frac{\mathrm{d}y_2}{\mathrm{d}t} &= dx_2(t)\left(y_2(t) + \kappa\alpha_1 y_1(t)\right) - \alpha_2 y_2(t).
\end{aligned} \tag{26}$$

The parameters $K_1, K_2, \mu_1, \mu_2, \alpha_1, \alpha_2, T_1, T_2,\ d, y_c,\ n$ and variables u_1, u_2 have the same meanings as in 2. Variables u_1 and u_2 - associated to biological processes duration T_1 and T_2 - are both ruled by an equation identical to 1. Parameters characterizing the UPR mechanism - threshold concentration y_c and sensivity n - are assumed to be identical for the two neurons. The UPR feedback function β_n is thus also identical for the two neurons.
We underline that neuron's proteins concentrations - (x_1, y_1) for neuron 1 and (x_2, y_2) for neuron 2 - are ruled by a system similar to 2 except that the interactions between PrP^{Sc} concentrations of the two neurons are now taken into account. Actually, we consider that diffusion enables the PrP^{Sc} proteins of one neuron to migrate near the other neuron and become templates for the generation of new PrP^{Sc} proteins. We decide to include these interactions in the PrP^{Sc} production terms: $dx_1\kappa\alpha_2 y_2$ (resp. $dx_2\kappa\alpha_1 y_1$) models the production of PrP^{Sc} proteins by neuron 1 (resp. 2) generated from the interaction between PrP^{Sc} proteins associated to neuron 2 (resp. 1) and PrP^{c} proteins of neuron 1 (resp. 2). Moreover we wish to grasp two properties: *(i)* isotropic and spatial properties of diffusion and *(ii)* possibly different interactions between PrP^{c} and PrP^{Sc} originating from different neurons compared to the situation where PrP^{c} and PrP^{Sc} come from the same neuron. Hence, we assume that the quantity of PrP^{Sc} that interacts - from one neuron to the other - decays with a factor $0 < \kappa \leq 1$. The parameter κ thus stands for a coupling constant between neurons that gathers both migration efficiency (induced by diffusion) and the ability for proteins originating from different neurons to interact.

The well-posedness of system 26 (existence, unicity and positivity of solutions) can be easily verified thanks to well-known theorems [37] (a result similar to 2.2 holds).

3.2 Steady states

Let $(x_1^*, x_2^*, y_1^*, y_2^*) \in \mathbb{R}_+^4$ be a steady state of 26, it verifies

$$0 = K_1\beta_n(y_1^*) - \mu_1 x_1^* - dx_1^*\left(y_1^* + \kappa\alpha_2 y_2^*\right), \tag{27}$$
$$0 = K_2\beta_n(y_2^*) - \mu_2 x_2^* - dx_2^*\left(y_2^* + \kappa\alpha_1\, y_1^*\right), \tag{28}$$
$$0 = dx_1^*\left(y_1^* + \kappa\alpha_2\, y_2^*\right) - \alpha_1\, y_1^*, \tag{29}$$
$$0 = dx_2^*\left(y_2^* + \kappa\alpha_1\, y_1^*\right) - \alpha_2 y_2^*. \tag{30}$$

Then, summing 27 with 29 and 28 with 30 we obtain

$$K_1\beta_n(y_1^*) - \mu_1 x_1^* - \alpha_1 y_1^* = 0 \text{ and } K_2\beta_n(y_2^*) - \mu_2 x_2^* - \alpha_2 y_2^* = 0,$$

which also reads, for $i, j \in \{1, 2\}$ and $i \neq j$:

$$x_i^* = G_i(y_i^*), \tag{31}$$

with

$$G_i(y) = \frac{1}{\mu_i}\left(K_i\beta_n(y) - \alpha_i y\right), \text{ for all } y \geq 0. \tag{32}$$

The function G_i is decreasing on $\mathbb{R}_+$ and non negative on $[0, \hat{y_i}]$ with

$$G_i(0) = \frac{K_i}{\mu_1} \text{ and } G_i(\hat{y_i}) = 0.$$

Now, inserting expression 31 into 29 and 30 leads to

$$y_1^* = y_2^* H_2(y_2^*), \tag{33}$$
$$y_2^* = y_1^* H_1(y_1^*), \tag{34}$$

where the function H_i for $i, j \in \{1, 2\}$, $i \neq j$ is defined as :

$$H_i(y) = \frac{1}{\kappa\alpha_j}\left(\frac{\alpha_i}{dG_i(y)} - 1\right), \text{ for all } y \in [0, \hat{y_i}).$$

Inserting expression 33 and 34 into each other leads to

$$y_1^* H_1(y_1^*)\, H_2\left(y_1^* H_1(y_1^*)\right) = y_1^*, \tag{35}$$
$$y_2^* H_2(y_2^*)\, H_1\left(y_2^* H_2(y_2^*)\right) = y_2^*. \tag{36}$$

Before going further, we underline that the function H_i (for $i, j \in \{1, 2\}$, $i \neq j$) is increasing on $[0, \hat{y_i})$ and such that

$$H_i(0) := \frac{1}{\kappa\alpha_j}\left(R_{0i}^{-1} - 1\right) \text{ and } \lim_{y \to \hat{y_i}} H_i(y) = +\infty, \tag{37}$$

where we define for further simplicity

$$R_{01} := \frac{dK_1}{\mu_1\alpha_1} \text{ and } R_{02} := \frac{dK_2}{\mu_2\alpha_2}.$$

We want to study existence and uniqueness of a possible co-existence steady state of 26, $(\bar{x}_1, \bar{x}_2, \bar{y}_1, \bar{y}_2) \in {\mathbb{R}_+^*}^4$, different from the trivial steady state $(K_1/\mu_1, K_2/\mu_2, 0, 0)$ (which always exists). We know that $(\bar{x}_1, \bar{x}_2, \bar{y}_1, \bar{y}_2)$ verifies 36. It follows that $\bar{y}_2 > 0$ is solution of

$$H(\bar{y}_2) = 1, \tag{38}$$

where the function H is defined as

$$H(y) = H_2(y) H_1\left(y H_2(y)\right),$$

for all $y \in (0, \hat{y}_2)$ in the domain of H. Depending on parameter values, $\bar{y}_2$ - solution of 38 - must lie in a given interval to ensure well-posedness of the

co-existence equilibria $(\bar{x}_1, \bar{x}_2, \bar{y}_1, \bar{y}_2)$. The three following Lemmas tackle this issue and unveil conditions about existence and uniqueness of the co-existence steady state $(\bar{x}_1, \bar{x}_2, \bar{y}_1, \bar{y}_2)$. If $R_{01} > 1$ and $R_{02} > 1$ then there exists a unique co-existence equilibrium $(\bar{x}_1, \bar{x}_2, \bar{y}_1, \bar{y}_2) \in {\mathbb{R}_+^*}^4$ verifying 31-33-34. By definition of H_1 of H_2, as $H_1(0), H_2(0) < 0$, there exist unique $\breve{y}_1, \breve{y}_2 > 0$ such that $H_1(\breve{y}_1) = 0$ and $H_2(\breve{y}_2) = 0$. Moreover, as $\bar{y}_2 > 0$ and $\bar{y}_1 > 0$, we know from equations 33 and 34 that we are looking for an equilibria $\bar{y}_2$, solution of 38 in $(\breve{y}_2, \hat{y}_2)$. In addition, we notice that $y \mapsto yH_2(y)$ is positive and increasing on $(\breve{y}_2, \hat{y}_2)$ and such that

$$\breve{y}_2 H_2(\breve{y}_2) = 0 \text{ and } \lim_{y \to \hat{y}_2} yH_2(y) = +\infty.$$

Hence, there exist unique $\tilde{\tilde{y}} < \tilde{y} \in (\breve{y}_2, \hat{y}_2)$ such that

$$\tilde{\tilde{y}} H_2(\tilde{\tilde{y}}) = \breve{y}_1 \text{ and } \tilde{y} H_2(\tilde{y}) = \hat{y}_1.$$

Consequently, $H_1(yH_2(y)) < 0$ and thus $H(y) < 0$ for all $y \in (\breve{y}_2, \tilde{y})$. And, by product and composition of positive increasing functions, H is positive, increasing on $\left[\tilde{\tilde{y}}, \tilde{y}\right)$ and such that $H(\tilde{\tilde{y}}) = 0$ and $\lim_{y \to \tilde{y}} H(y) = +\infty$. All in all, if $R_{01} > 1$ and $R_{02} > 1$ then there exists a unique solution $\bar{y}_2 \in \left(\tilde{\tilde{y}}, \tilde{y}\right)$ of equation 38 and 3.2 is proven. Then, we focus on the situation in which only one neuron has its R_0 greater than one.

If $R_{0i} > 1$ and $R_{0j} < 1$ with $i, j \in \{1, 2\}$ and $i \neq j$, then there exists a unique co-existence equilibrium $(\bar{x}_1, \bar{x}_2, \bar{y}_1, \bar{y}_2) \in {\mathbb{R}_+^*}^4$ verifying 31-33-34. For simplicity and without loss of generality, we assume that $i = 2$ and $j = 1$. By definition of H_2, we know that $H_2(0) < 0$ and from the increasing property of H_2, we obtain that there exists a unique $\breve{y}_2 \in (0, \hat{y_2})$ such that $H_2(\breve{y}_2) = 0$. Moreover from equations 33 and 34, since $\bar{y_1} > 0$, it is necessary that $\bar{y_2} \in (\breve{y}_2, \hat{y_2})$. From equations 35 and 36, we are consequently looking for a solution $\bar{y_2} \in (\breve{y}_2, \hat{y_2})$ of 38. By the increasing properties of H_1 and H_2 and by the positiveness of H_1 on its domain, we know that H is positive and increasing on $(\breve{y}_2, \hat{y_2})$ and such that

$$H(\breve{y}_2) = 0 \text{ and } \lim_{y \to \hat{y_2}} H(y) = +\infty.$$

All in all, if $R_{02} > 1$ and $R_{01} < 1$, then there exists a unique solution $\bar{y_2} \in (\breve{y}_2, \hat{y_2})$ to equation 38 and 3.2 is proven.

Assume that

$$R_{01} < 1 \text{ and } R_{02} < 1. \tag{39}$$

There exists another unique co-existence equilibrium $(\bar{x}_1, \bar{x}_2, \bar{y}_1, \bar{y}_2) \in {\mathbb{R}_+^*}^4$ verifying 31-33-34 if and only if

$$\kappa^2 > \frac{1}{R_{01} R_{02} \alpha_1 \alpha_2} \left[1 - R_{01}\right] \left[1 - R_{02}\right]. \tag{40}$$

First we know from the definition of H_2 that there exists a unique $\tilde{y} \leq \hat{y_2}$ such that

$$\tilde{y} H_2(\tilde{y}) = \hat{y_1}.$$

Then conditions $R_{01} < 1$ and $R_{02} < 1$ implies the positiveness of H_1, H_2 and $y \mapsto H_1(yH_2(y))$ on $(0, \tilde{y})$. By operations, H is thus well defined and increasing on its domain $(0, \tilde{y})$ and such that

$$\lim_{y \to \tilde{y}} H(y) = +\infty \text{ and } H(0) = \frac{1}{\kappa^2 \alpha_1 \alpha_2} \left[R_{01}^{-1} - 1\right] \left[R_{02}^{-1} - 1\right].$$

All things considered, when condition 39 holds, the co-existence equilibrium $(\bar{x}_1, \bar{x}_2, \bar{y}_1, \bar{y}_2)$ with $\bar{y}_2 > 0$ verifiying equation 38 exists and is unique if and only if condition 40 holds (*i.e* $H(0) < 1$). This concludes the proof.

We summarize the results in the following Theorem. The system 26 always admits a trivial equilibrium $\left(\frac{K_1}{\mu_1}, \frac{K_2}{\mu_2}, 0, 0\right)$. Moreover, there exists another unique co-existence equilibrium $(\bar{x}_1, \bar{x}_2, \bar{y}_1, \bar{y}_2) \in {\mathbb{R}_+^*}^4$ verifying equations 31-33-34 if and only if

(i)

$$R_{01} < 1,\ R_{02} < 1 \text{ and } \kappa^2 > \frac{1}{R_{01} R_{02} \alpha_1 \alpha_2} \left[1 - R_{01}\right] \left[1 - R_{02}\right], \quad (41)$$

or

(ii) there exists $i \in \{1, 2\}$ such that $R_{0i} > 1$.

If we denote by

$$R_{00} = \kappa^2 \alpha_1 \alpha_2 \frac{R_{01} R_{02}}{\left[1 - R_{01}\right] \left[1 - R_{02}\right]}, \quad (42)$$

we can see that the existence of the co-existence equilibrium is equivalent to $R_{01} < 1$, $R_{02} < 1$ and $R_{00} > 1$, or there exists $i \in \{1, 2\}$ such that $R_{0i} > 1$. The main information here is that even if R_{01} and R_{02} of each neuron is less than 1, a large coupling constant κ between the two neurons allows R_{00} of the coupling to be greater than 1.

Finally, we state and prove a result concerning the continuous differentiability of the co-existence steady state with respect to the coupling parameter κ. Assume that there exists $i \in \{1, 2\}$ such that $R_{0i} > 1$. The co-existence steady state $(\bar{x}_1, \bar{x}_2, \bar{y}_1, \bar{y}_2)$ is a continuously differentiable function of κ on an open set $U \subset \mathbb{R}^+$ with $0 \in U$, if and only if

$$K_i \beta_n'(\bar{y_i}) - \alpha_i > 0 \text{ for } i \in \{1, 2\} \text{ such that } R_{0i} > 1.$$

The system composed of steady-state equations 27 - 28 - 29 - 30 could also be written $F(\kappa, (x_1^*, x_2^*, y_1^*, y_2^*)) = 0$ where $F : \mathbb{R}_+ \times \mathbb{R}_+^4 \to \mathbb{R}$. Let $J_F(\kappa, (x_1^*, x_2^*, y_1^*, y_2^*))$ be the jacobian determinant of F with respect to its second variable in $\mathbb{R}_+^4$. In this framework, simple computations lead to :

$$J_F(\kappa, (x_1^*, x_2^*, y_1^*, y_2^*)) =$$
$$\begin{vmatrix} -(\mu_1 + d y_1^* + d\kappa\alpha_2 y_2^*) & 0 & K_1\beta_n'(y_1^*) - d x_1^* & -d x_1^* \kappa\alpha_2 \\ 0 & -(\mu_2 + d y_2^* + d\kappa\alpha_1 y_1^*) & -d x_2^* \kappa\alpha_1 & K_2\beta_n'(y_2^*) - d x_2^* \\ d(y_1^* + \kappa\alpha_2 y_2^*) & 0 & d x_1^* - \alpha_1 & d x_1^* \kappa\alpha_2 \\ 0 & d(y_2^* + \kappa\alpha_1 y_1^*) & d x_2^* \kappa\alpha_1 & d x_2^* - \alpha_2 \end{vmatrix}. \quad (43)$$

For clarity, we note $(\bar{x_1}_\kappa, \bar{x_2}_\kappa, \bar{y_1}_\kappa, \bar{y_2}_\kappa)$ the co-existence steady state of system 26 for $\kappa \in [0,1]$.

We want to apply the implicit function theorem at $\kappa = 0$ and thus need to evaluate J_F in the co-existence steady state obtained for the decorrelated situation ($\kappa = 0$). However, in the decorrelated situation, since $\kappa = 0$, we notice that $(\bar{x_1}_{\kappa=0}, \bar{y_1}_{\kappa=0})$ and $(\bar{x_2}_{\kappa=0}, \bar{y_2}_{\kappa=0})$ are steady states of neuron 1 and 2 independently. Consequently, depending on the values of R_{01} and R_{02} with respect to 1, two different situations must be distinguished.

First, if $R_{01} > 1$ and $R_{02} > 1$ then condition 4 is satisfied for each neuron. We thus know that $\bar{x_1}_{\kappa=0} = \alpha_1/d$ and $\bar{x_2}_{\kappa=0} = \alpha_2/d$ and that $\bar{y_1}_{\kappa=0}$ and $\bar{y_2}_{\kappa=0}$ verify equations similar to equation 5. These expressions and a Laplace expansion of 43 leads to

$$J_F\left(0, (\bar{x_1}_{\kappa=0}, \bar{x_2}_{\kappa=0}, \bar{y_1}_{\kappa=0}, \bar{y_2}_{\kappa=0})\right) = d^2 \bar{y_1}_{\kappa=0} \bar{y_2}_{\kappa=0} \left[K_1 \beta_n'(\bar{y_1}_{\kappa=0}) - \alpha_1\right] \left[K_2 \beta_n'(\bar{y_2}_{\kappa=0}) - \alpha_2\right].$$

This expression and the implicit function theorem enable us to conclude for the situation in which $R_{01} > 1$ and $R_{02} > 1$.

Then, let $i, j \in \{1,2\}$, $i \neq j$ and assume that $R_{0i} > 1$ and $R_{0j} < 1$. Without loss of generality and for clarity, we assume that $R_{01} > 1$ and $R_{02} < 1$. In this situation, we thus have $\bar{x_2}_{\kappa=0} = K_2/\mu_2$, $\bar{y_2}_{\kappa=0} = 0$, $\bar{x_1}_{\kappa=0} = \alpha_1/d$ and $\bar{y_1}_{\kappa=0}$ verifies equation 5 (with parameters adapted to neuron 1). Hence, from these expressions and with a Laplace expansion of 43 we obtain

$$J_F\left(0, (\bar{x_1}_{\kappa=0}, \bar{x_2}_{\kappa=0}, \bar{y_1}_{\kappa=0}, \bar{y_2}_{\kappa=0})\right) = d\mu_2\alpha_2 \left(R_{02} - 1\right) \bar{y_1}_{\kappa=0} \left[K_1 \beta_n'(\bar{y_1}_{\kappa=0}) - \alpha_1\right].$$

Using the latter expression and the implicit function theorem, if $R_{01} > 1$ and $R_{02} < 1$, we conclude that $(\bar{x}_1, \bar{x}_2, \bar{y}_1, \bar{y}_2)$ is continuous and differentiable with respect to κ in an open set $U \subset {\mathbb{R}_+^*}^4$ containing $\kappa = 0$ if and only if $K_1 \beta_n'(\bar{y_1}_{\kappa=0}) - \alpha_1 \neq 0$.

Proof of 3.2 is thus completed.

When $\kappa = 0$, each neuron is expected to evolve independently from the other and to have its own prion dynamics. 3.2 thus guarantees the coherence with our previous modelling of a single neuron and ensures the well-posedness of our model.

When neurons are identical (*i.e.* symmetrical situation), more precise theoretical results become simpler. 3.2 leads to the following corollary.

If neurons are identical with $K := K_1 = K_2$, $\mu := \mu_1 = \mu_2$ and $\alpha := \alpha_1 = \alpha_2$, then system 26 admits a unique co-existence steady state $(\bar{x}_1, \bar{x}_2, \bar{y}_1, \bar{y}_2)$ if and only if

$$\kappa > \frac{1 - R_0}{\alpha R_0} \text{ with } R_0 := R_{01} = R_{02} = \frac{dK}{\mu\alpha}. \tag{44}$$

If 44 holds, we have

$$\bar{x} := \bar{x}_1 = \bar{x}_2 = \frac{\alpha}{d(1 + \kappa\alpha)},$$

and $\bar{y} := \bar{y}_1 = \bar{y}_2 \in (0, \hat{y})$ solution of

$$R_0 \beta_n(\bar{y}) = \frac{d}{\mu}\bar{y} + \frac{1}{1 + \kappa\alpha},\ \bar{y} \in (0, \hat{y}). \tag{45}$$

If neurons are identical, the condition $\kappa > (1 - R_0)/\alpha R_0$ is in fact equivalent to $R_{00} := [\kappa\alpha R_0/(1 - R_0)]^2 > 1$. By symmetry we have $x_1^* = x_2^* := x^*$ and

$y_1^* = y_2^* := y^*$. Hence, inserting the latter equality in equations 33 and 34 leads to

$$y^* = y^* h(y^*),$$

where $h := H_1 = H_2$ in the symmetrical situation under consideration here. As $x^* > 0$ and $y^* > 0$, it is necessary that $y^* < K/\alpha$. Hence, existence and uniqueness of a co-existence steady state $y^* \in [0, \hat{y})$ relies on the solution of

$$1 = h(y) = \frac{1}{\kappa\alpha}\left(\frac{\alpha\mu}{d(K\beta_n(y) - \alpha y)} - 1\right), y \in [0, \hat{y}),$$

which corresponds to equation 45. Function h being increasing on $[0, \hat{y})$ and such that $\lim_{y\to\hat{y}} h(y) = +\infty$, we consequently obtain existence and uniqueness of the co-existence steady state (x^*, x^*, y^*, y^*) if and only if $h(0) < 1$. This condition is also equivalent to 44. Finally, a trivial solving of equation 31 leads to an explicit expression of x^*.

3.3 Linearised system, characteristic equation and asymptotic stability

System 26 linearised with the perturbations u_1, u_2, u_3 and u_4 about any steady state $(x_1^*, x_2^*, y_1^*, y_2^*)$, reads

$$\begin{aligned}
\frac{\mathrm{d}u_1}{\mathrm{d}t} &= K_1\beta_n'(y_1^*)u_3(t-T_1) - (\mu_1 + dy_1^* + d\kappa\alpha_2 y_2^*)u_1(t) - dx_1^* u_3(t) - d\kappa\alpha_2 x_1^* u_4(t),\\
\frac{\mathrm{d}u_2}{\mathrm{d}t} &= K_2\beta_n'(y_2^*)u_4(t-T_2) - (\mu_2 + dy_2^* + d\kappa\alpha_1 y_1^*)u_2(t) - d\kappa\alpha_1 x_2^* u_3(t) - dx_2^* u_4(t),\\
\frac{\mathrm{d}u_3}{\mathrm{d}t} &= (dy_1^* + d\kappa\alpha_2 y_2^*)u_1(t) + (dx_1^* - \alpha_1)u_3(t) + d\kappa\alpha_2 x_1^* u_4(t),\\
\frac{\mathrm{d}u_4}{\mathrm{d}t} &= (dy_2^* + d\kappa\alpha_1 y_1^*)u_2(t) + d\kappa\alpha_1 x_2^* u_3(t) + (dx_2^* - \alpha_2)u_4(t),
\end{aligned}$$

from which we deduce, the associated characteristic equation for $\lambda \in \mathbb{C}$:

$$\begin{vmatrix}
W_1(\lambda) & 0 & dx_1^* - K_1\beta_n'(y_1^*)\mathrm{e}^{-\lambda T_1} & d\kappa\alpha_2 x_1^* \\
0 & W_2(\lambda) & d\kappa\alpha_1 x_2^* & dx_2^* - K_2\beta_n'(y_2^*)\mathrm{e}^{-\lambda T_2} \\
-(dy_1^* + d\kappa\alpha_2 y_2^*) & 0 & \lambda + \alpha_1 - dx_1^* & -d\kappa\alpha_2 x_1^* \\
0 & -(dy_2^* + d\kappa\alpha_1 y_1^*) & -d\kappa\alpha_1 x_2^* & \lambda + \alpha_2 - dx_2^*
\end{vmatrix} = 0. \tag{46}$$

where we defined, for $i, j \in \{1, 2\}$, $i \neq j$:

$$W_i(\lambda) = \lambda + \mu_i + dy_i^* + d\kappa\alpha_j y_j^*.$$

The trivial steady state is the only steady state and locally asymptotically stable if and only if

$$R_{01} < 1,\ R_{02} < 1,\ \text{and } 0 \leq \kappa^2 < \frac{1}{R_{01}R_{02}\alpha_1\alpha_2}\left[1 - R_{01}\right]\left[1 - R_{02}\right]. \tag{47}$$

Otherwise, the trivial steady is unstable. Using the notation 42, we can see that the condition 47 is equivalent to $R_{0i} < 1$, for all $i \in \{0, 1, 2\}$. For the trivial steady-state, the characteristic equation 46 reads

$$(\lambda+\mu_1)(\lambda+\mu_2)\left[\left(\lambda + \alpha_1 - \frac{dK_1}{\mu_1}\right)\left(\lambda + \alpha_2 - \frac{dK_2}{\mu_2}\right) - \frac{d^2\kappa^2 K_1 K_2 \alpha_1}{\mu_1\mu_2}\right] = 0, \quad \lambda \in \mathbb{C}.$$

Thus, we have at least two eigenvalues $-\mu_1 < 0$ and $-\mu_2 < 0$. Others possible eigenvalues verify

$$\lambda^2 + \left(\alpha_1 + \alpha_2 - d\left(\frac{K_1}{\mu_1} + \frac{K_2}{\mu_2}\right)\right)\lambda + \left(\alpha_1 - \frac{dK_1}{\mu_1}\right)\left(\alpha_2 - \frac{dK_2}{\mu_2}\right) - \frac{d^2\kappa^2 K_1 K_2 \alpha_1 \alpha_2}{\mu_1 \mu_2} = 0, \quad \lambda \in \mathbb{C}.$$

From the Routh-Hurwtiz criterion, it follows that this equation has roots with negative real parts if and only if

$$\alpha_1(1 - R_{01}) + \alpha_2(1 - R_{02}) > 0 \text{ and } \left(\alpha_1 - \frac{dK_1}{\mu_1}\right)\left(\alpha_2 - \frac{dK_2}{\mu_2}\right) - \frac{d^2\kappa^2 K_1 K_2 \alpha_1 \alpha_2}{\mu_1 \mu_2} > 0,$$

which is also equivalent to

$$\alpha_1(1 - R_{01}) + \alpha_2(1 - R_{02}) > 0 \text{ and } \frac{1}{R_{01}R_{02}\alpha_1\alpha_2}[1 - R_{01}][1 - R_{02}] > \kappa^2.$$

As $\kappa^2 \geq 0$, the latter conditions is finally equivalent to condition 47.

Interchanging lines and columns and using 2×2 block matrices, the characteristic equation 46 reads

$$\begin{vmatrix} A_1(\lambda) & B_1 \\ B_2 & A_2(\lambda) \end{vmatrix} = 0, \ \lambda \in \mathbb{C}, \tag{48}$$

with, for $i, j \in \{1, 2\}$, $i \neq j$:

$$A_i(\lambda) = \begin{pmatrix} W_i(\lambda) & dx_i^* - K_i\beta_n'(y_i^*)\mathrm{e}^{-\lambda T_i} \\ -dy_i^* - d\kappa\alpha_j y_j^* & \lambda + \alpha_i - dx_i^* \end{pmatrix} \text{ and } B_i = d\kappa\alpha_j x_i^* \begin{pmatrix} 0 & 1 \\ 0 & -1 \end{pmatrix}.$$

In order to obtain theoretical result, we decide to consider the symmetrical situation in which neurons are identical with $T := T_1 = T_2$. In such situation, for any steady state (x^*, x^*, y^*, y^*), the characteristic equation 48 reads:

$$\begin{vmatrix} A(\lambda) & B \\ B & A(\lambda) \end{vmatrix} = 0, \ \lambda \in \mathbb{C},$$

where

$$A(\lambda) := A_1(\lambda) = A_2(\lambda) \text{ and } B := B_1 = B_2.$$

Hence, in the symmetrical situation, the characteristic equation for the coexistence steady state $(\bar{x}, \bar{x}, \bar{y}, \bar{y}) \in {\mathbb{R}_+^*}^4$ is a product of two second order polynomials :

$$\det(A(\lambda) + B)\det(A(\lambda) - B) = 0, \ \lambda \in \mathbb{C}, \tag{49}$$

where, after simple computations using results of 3.2, we have

$$\begin{aligned} \det(A(\lambda) + B) = {} & \lambda^2 + [\mu R_0(1 + \kappa\alpha)\beta_n(\bar{y})]\lambda - \alpha\mu[1 - R_0(1 + \kappa\alpha)\beta_n(\bar{y})] \\ & + K\beta_n'(\bar{y})\mu[1 - R_0(1 + \kappa\alpha)\beta_n(\bar{y})]\mathrm{e}^{-\lambda T}, \end{aligned} \tag{50}$$

and

$$\begin{aligned}\det\left(A(\lambda)-B\right) &= \lambda^2+\left[\mu R_0(1+\kappa\alpha)\beta_n(\bar{y})+\frac{2\kappa\alpha^2}{1+\kappa\alpha}\right]\lambda \\ &\quad +2\frac{\kappa\alpha^2}{1+\kappa\alpha}\mu R_0(1+\kappa\alpha)\beta_n(\bar{y})-\frac{\alpha(1-\kappa\alpha)}{1+\kappa\alpha}\mu\left[1-R_0(1+\kappa\alpha)\beta_n(\bar{y})\right] \\ &\quad +K\beta_n'(\bar{y})\mu\left[1-R_0(1+\kappa\alpha)\beta_n(\bar{y})\right]\mathrm{e}^{-\lambda T}.\end{aligned} \tag{51}$$

Now, we state and prove some results about the local asymptotic stability of the co-existence steady state in the situation of identical neurons (*i.e.* symmetrical situation).

If

(i) neurons are identical with $K := K_1 = K_2$, $\alpha := \alpha_1 = \alpha_2$ and $\mu := \mu_1 = \mu_2$,

(ii) $\kappa > \dfrac{1-R_0}{\alpha R_0}$ (condition equivalent to $R_{00} > 1$),

(iii) $T_1 = T_2 = 0$,

then the co-existence steady state $(\bar{x},\bar{x},\bar{y},\bar{y}) \in {\mathbb{R}_+^*}^4$ is locally asymptotically stable. If $T_1 = T_2 = 0$, then the two terms 50 and 51 of the characteristic equation 49 read (computations are not shown for clarity) for $\lambda \in \mathbb{C}$:

$$\det\left(A(\lambda)+B\right) = \lambda^2+\left[\mu R_0(1+\kappa\alpha)\beta_n(\bar{y})\right]\lambda-\left(\alpha-K\beta_n'(\bar{y})\right)\mu\left[1-R_0(1+\kappa\alpha)\beta_n(\bar{y})\right],$$

and

$$\begin{aligned}\det\left(A(\lambda)-B\right) &= \lambda^2+\left[\mu R_0(1+\kappa\alpha)\beta_n(\bar{y})+2\frac{\kappa\alpha^2}{1+\kappa\alpha}\right]\lambda \\ &\quad +\frac{\kappa\alpha^2}{1+\kappa\alpha}\left[\mu R_0(1+\kappa\alpha)\beta_n(\bar{y})+\mu\right] \\ &\quad -\left(\frac{\alpha}{1+\kappa\alpha}-K\beta_n'(\bar{y})\right)\mu\left[1-R_0(1+\kappa\alpha)\beta_n(\bar{y})\right].\end{aligned}$$

From the results obtained in 3.2, from the positiveness of $\bar{y}$ and from the decreasing shape of β_n, we verify that $1-R_0(1+\kappa\alpha)\beta_n(\bar{y}) < 0$ and thus obtain that each factors of the two latter polynomials are positive. Hence, we conclude using the Routh-Hurwitz criterion applied to the two latter polynomials.

From 3.3, we use a continuity argument to obtain the following corollary. If conditions (i) and (ii) of 3.3 hold and $T := T_1 = T_2$, then there exists a unique $T^* \in (0,+\infty)$ such that the co-existence steady state $(\bar{x},\bar{x},\bar{y},\bar{y}) \in {\mathbb{R}_+^*}^4$ is locally asymptotically stable for all $T < T^*$ and unstable for $T \geq T^*$ at the neighborhood of T^*.

If T is increased from 0 to $+\infty$ with fixed values of other model parameters, the system of two identical neurons can undergo a stability switch through a Hopf bifurcation when T reaches T^*.

Similarly to what has been done for a single neuron, we used the method detailed in [14] to determine theoretical conditions and expressions of the boundary delays at which stability switches could occur. For different values of $\kappa \in [0,1]$,

we thus numerically obtained the corresponding values of T^* at which a Hopf bifurcation could occur.
In 4, we present stability diagrams (4a and 4c) and illustrate the stability switch that could occur when $R_0 > 1$ and $R_0 < 1$ through two different plots (4b and 4d). These figures highlight the influence of the coupling between the two neurons over the stability of the co-existence steady state. The more important is the coupling, the smaller is the boundary value of T at which a stability switch occurs. As observed in stability diagrams, neuron coupling ($\kappa > 0$) actually promotes instability by lowering the value of the biological processes duration T^* at which a stability switch occurs compared to the situation without coupling ($\kappa = 0$, single neuron).

Because of the lack of referenced biological values we chose model parameters values according to relevant order magnitudes following previous modelling works [17, 23]. Yet, the threshold concentration y_c was chosen arbitrarily. The value of the sensitivity coefficient n significantly influences the time complexity of simulations. Thus, we chose the value $n = 10$ as a compromise between a reasonable computational time complexity and reasonable sharpness of the UPR feedback function β_n. Finally, the value of R_0 (either greater or lower than 1) was set by adjusting the value of α.

Table 2: Values of parameters used in 4. Orders of magnitude are consistent with the values used in [17, 23].

Parameters	Values	Units
T	variable (4a and 4c) or 0.15 (4d)	days
$\mu_1 = \mu_2 = \mu$	20	days^{-1}
$K_1 = K_2 = K$	1500	(Fibrils per volume unit).days^{-1}
$\alpha_1 = \alpha_2 = \alpha$	2.0833 (4a and 4b) or 4.6875 (4c and 4d)	days^{-1}
κ	variable (4a, 4c and 4d) or 0.2 (4b)	-
y_c	130	Fibrils per volume unit
d	0.05	(Fibrils per volume unit)$^{-1}$.days^{-1}
n	10	-

4 Discussion and conclusion

The formalism we used to depict prion dynamics with two neurons can be easily generalized to describe prion dynamics in a system of N neurons. Doing so, we obtain a model similar to the one developed by Stumpf and Krakauer [42], except our approach incorporates the UPR feedback and do not assume preferential diffusion along axons.
In this paradigm, each neuron $i \in [\![1, N]\!]$ is modeled with its associated PrP^c

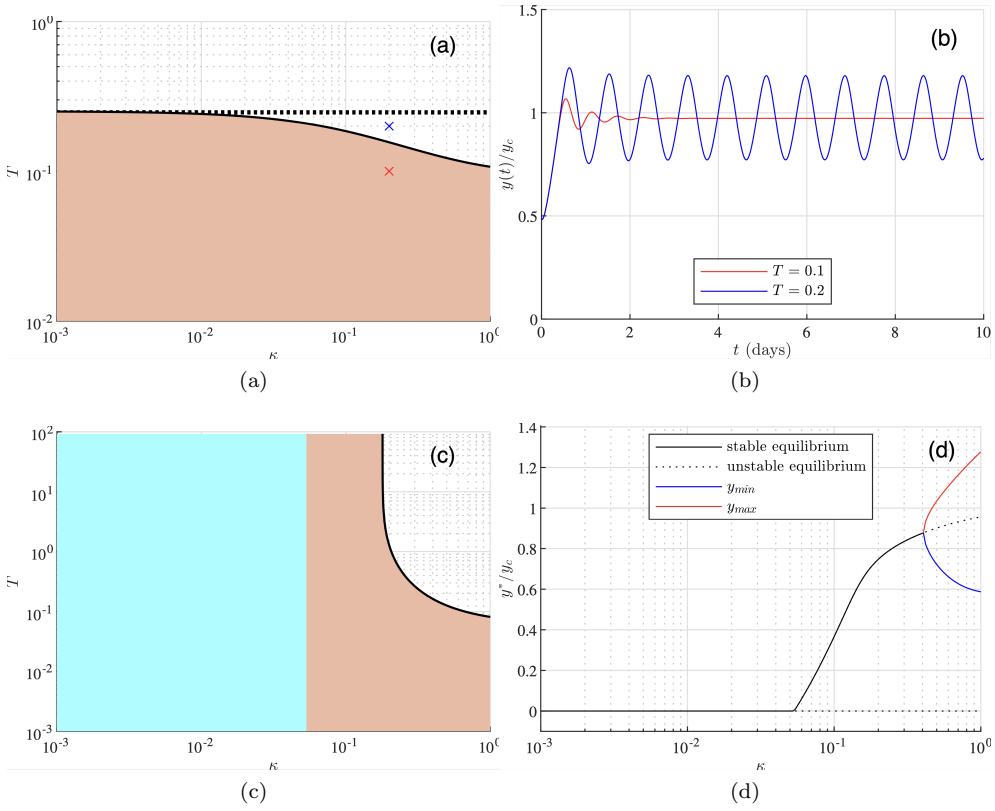

Figure 4: **(a)**, **(c)** : Stability diagrams in the (κ, T) plane when neurons are strictly identical with $R_0 > 1$ **(a)** or $R_0 < 1$ **(c)**. Full lines locate T^*: the first crossing of the imaginary axis by the characteristic roots associated to the co-existence steady state. It corresponds to the first value of T (when increased from 0) that induces a stability switch through a Hopf bifurcation. Colored areas indicate stability regions for the trivial (blue) or co-existence (red) steady states. In **(a)**, that is $R_0 > 1$, we also highlight by a dashed line the value of T^* obtained for the model of a single neuron (presented in 2). We verify the coherence between the two models as $\kappa \to 0$ and observe the effect of neuron coupling: the boundary value T^* decreases with κ. Neuron coupling thus promote instability. In **(c)**, that is $R_0 < 1$, if κ is small enough, the disease free equilibrium is the only steady state but also asymptotically stable. However, when coupling parameter κ is large enough, the disease steady state eventually appears and becomes also stable. This means that even with $R_0 < 1$, the coupling allows the disease to play a major role. **(b)**: Example trajectories when $R_0 > 1$ illustrating the Hopf bifurcation that occurs when T crosses the boundary. Trajectories are colored according to their parameter values and correspond to the colored crosses of 4a. **(d)** Evolution of normalized PrP^{Sc} steady state values y^*/y_c with respect to the coupling constant κ when $R_0 < 1$. For a given value of κ, then there is one or two steady states which can be stable (full line) or unstable (dashed line). When there are 2 unstable steady states, the solution is periodic and we indicate its maximum and minimum with red and blue lines, respectively. Values of other model parameters (specified in 2) are set to relevant orders of magnitudes.

and PrP^{Sc} concentrations x_i and y_i ruled by

$$\frac{\mathrm{d}x_i}{\mathrm{d}t} = K_i\beta_n(y_i(t-T_1)) - \mu_i x_i(t) - dx_i\left(y_i(t) + \sum_{j\neq i}\kappa_{i,j}\alpha_{j\to i}y_j(t)\right),$$

$$\frac{\mathrm{d}y_i}{\mathrm{d}t} = dx_i(t)\left(y_i(t) + \sum_{j\neq i}\kappa_{i,j}\alpha_{j\to i}y_j(t)\right) - \left(\sum_{j\neq i}\alpha_{i\to j}\right)y_2(t).$$

Parameters d, K_i and μ_i have the same meaning as before concerning neuron $i \in [\![1, N]\!]$. The parameter $\alpha_{i\to j}$ transcribes the diffusive property of PrP^{Sc} to the neuron $j \neq i$. We still assume that interactions between PrP^{Sc} from neuron i to PrP^{C} of an other neuron $j \neq i$ is modeled with a coupling factor $0 \leq \kappa_{i,j} < 1$. We remind that these coupling constants should be viewed as damping coefficients characterizing both diffusion properties and difference of origin between prion species.

In conclusion, we developed a modeling approach of prion production at the scale of one (2) or two (3) neurons. Our approach incorporates the effect of the Unfolded Protein Response through a negative feedback describing the global translation shutdown induced by an overload of PrP^{Sc} around a neuron.

We investigated existence, uniqueness and (local) stability of steady states associated to each of the two models presented in this paper. In these models, a bifurcation analysis with respect to the variation of three parameter (for the single neuron's prion model) or a continuity argument (for the two neuron's model) led to condition for autonomous oscillations of PrP^{Sc} to appear. Stability diagrams and numerical simulations gave us insight in the stability of steady states as well as in the dynamics of solutions. In the case of two neurons, we established - both theoretically and numerically - an interesting result. Interactions between PrP^{Sc} and PrP^{c} originating from different neurons enable - if the coupling constant κ is greater than a minimum value - existence and uniqueness of a co-existence steady state (and possibly PrP^{Sc} oscillations to appear) even when the R_0 associated to each single neuron[4] is lower than one. Theoretical results and numerical simulations concerning the case of 2 identical neurons indicate that the value of κ dictates prion dynamics at the scale of two neurons and show that the co-existence steady state could be destabilized - inducing PrP^{Sc} oscillations - when the biological processes duration T excesses a boundary value T^*.

Even if, our models aim at describing PrP^{c} and PrP^{Sc} concentrations around neurons, future research may extend and/or modify our modeling approach to describe concentrations of different misfolded proteins involved in other Protein Misfolding Disorders, such as Aβ proteins in the context of Alzheimer's Disease.

Moreover, by considering the effect of a global translation shutdown at the neuron scale (through protein synthesis activity and biological activity variables), our model paves the way for future investigations into the effect of neuron synchronization in prion diseases. Actually, this work constitutes the building block of a future wider modeling approach in which neurons could interact through PrP^{Sc} diffusion and possibly oscillates (depending on their environment and biological parameters) and then potentially see their protein synthesis activities become synchronized thus triggering detrimental outcomes.

[4] characterizing existence and uniqueness of the endemic steady state

To this aim, we will have to take several important physiological features of the neuronal network into account. Indeed, since prion proteins are anchored to the cell membrane, the PrP^{Sc} formation follows the synaptic entanglement and thus do not propagate equally in all directions. Thus, some of the neurons not located in the neighborhood of a stressed one, could be impacted by its behavior and propagate the UPR mechanism in an unexpected heterogeneous way. Furthermore, similarly to a group of persons tied together and trying to figure out how to progress in a jungle, diffusion coefficient of PrP^{Sc} proteins depends mainly on the on its size (called the polymer length). The longer the protein is, the less it diffuses. And thus, secondary nucleation could appear far from the source of the onset of the pathology in a group of neurons if polymers of small sizes are produced in a sufficient quantity. Then, the synchronicity could be described either through a local connection in standard but technical way, or through an unexpected non local heterogeneous way. This has to be clearly observed *in vivo* through image analysis, and described with new mathematical models and technical approaches. This is the object of our future but promising work.

References

[1] Yves Achdou, Bruno Franchi, Norina Marcello, and Maria Carla Tesi. A qualitative model for aggregation and diffusion of β-amyloid in Alzheimer's disease. *Journal of Mathematical Biology*, 67(6):1369–1392, December 2013.

[2] Mostafa Adimy and Fabien Crauste. Modelling and Asymptotic Stability of a Growth Factor-Dependent Stem Cells Dynamics Model with Distributed Delay. *Discrete and Continuous Dynamical Systems - Series B*, 8(1):19–38, 2007.

[3] Martin Andrade-Restrepo, Ionel Sorin Ciuperca, Paul Lemarre, Laurent Pujo-Menjouet, and Léon Matar Tine. A reaction–diffusion model of spatial propagation of A β oligomers in early stage Alzheimer's disease. *Journal of Mathematical Biology*, 82(5):39, March 2021.

[4] Martin Andrade-Restrepo, Paul Lemarre, Laurent Pujo-Menjouet, Leon Matar Tine, and Sorin Ionel Ciuperca. Modeling the spatial propagation of Aβ oligomers in Alzheimer's Disease. *ESAIM: ProcS*, 67:30–45, 2020.

[5] Edoardo Beretta and Yang Kuang. Geometric Stability Switch Criteria in Delay Differential Systems with Delay Dependent Parameters. *SIAM J. Math. Anal.*, 33(5):1144–1165, January 2002.

[6] Michiel Bertsch, Bruno Franchi, Norina Marcello, Maria Carla Tesi, and Andrea Tosin. Alzheimer's disease: a mathematical model for onset and progression. *Mathematical Medicine and Biology: A Journal of the IMA*, 34(2):193–214, June 2017.

[7] Michiel Bertsch, Bruno Franchi, Maria Carla Tesi, and Andrea Tosin. Microscopic and macroscopic models for the onset and progression of Alzheimer's disease. *Journal of Physics A: Mathematical and Theoretical*, 50(41):414003, September 2017.

[8] V. Calvez, N. Lenuzza, M. Doumic, J-P Deslys, F. Mouthon, and B. Perthame. Prion dynamics with size dependency–strain phenomena. *Journal of Biological Dynamics*, 4(1):28–42, January 2010.

[9] Vincent Calvez, Natacha Lenuzza, Dietmar Oelz, Jean-Philippe Deslys, Pascal Laurent, Franck Mouthon, and Benoît Perthame. Size distribution dependence of prion aggregates infectivity. *Mathematical Biosciences*, 217(1):88–99, January 2009.

[10] Felix Carbonell, Yasser Iturria-Medina, and Alan C. Evans. Mathematical Modeling of Protein Misfolding Mechanisms in Neurological Diseases: A Historical Overview. *Frontiers in Neurology*, 9:37, 2018.

[11] Monique Chyba, Jakob Kotas, Vincent Beringue, Christopher Eblen, Angelique Igel-Egalon, Yuliia Kravchenko, and Human Rezaei. An alternative model to prion fragmentation based on the detailed balance between PrP^{sc} and suPrP. *bioRxiv*, page 2020.04.24.058917, January 2020.

[12] Katherine L. Cook, Pamela A. G. Clarke, Jignesh Parmar, Rong Hu, Jessica L. Schwartz-Roberts, Mones Abu-Asab, Anni Wärri, William T. Baumann, and Robert Clarke. Knockdown of estrogen receptor-α induces autophagy and inhibits antiestrogen-mediated unfolded protein response activation, promoting ROS-induced breast cancer cell death. *The FASEB Journal*, 28(9):3891–3905, September 2014.

[13] Hans Engler, Jan Prüss, and Glenn F. Webb. Analysis of a model for the dynamics of prions II. *Journal of Mathematical Analysis and Applications*, 324(1):98–117, December 2006.

[14] Guihong Fan, Maung Min-Oo, and Gail Wolkowicz. HOPF BIFURCATION OF DELAY DIFFERENTIAL EQUATIONS WITH DELAY DEPENDENT PARAMETERS. *The Canadian Applied Mathematics Quarterly*, 17(1), January 2009.

[15] Joseph C Genereux, Song Qu, Minghai Zhou, Lisa M Ryno, Shiyu Wang, Matthew D Shoulders, Randal J Kaufman, Corinne I Lasmézas, Jeffery W Kelly, and R Luke Wiseman. Unfolded protein response-induced ERdj3 secretion links ER stress to extracellular proteostasis. *The EMBO Journal*, 34(1):4–19, January 2015.

[16] Joseph C Genereux and R Luke Wiseman. Regulating extracellular proteostasis capacity through the unfolded protein response. *Prion*, 9(1):10–21, January 2015.

[17] Meredith L. Greer, Laurent Pujo-Menjouet, and Glenn F. Webb. A mathematical analysis of the dynamics of prion proliferation. *Journal of Theoretical Biology*, 242(3):598–606, October 2006.

[18] Claudio Hetz and Bertrand Mollereau. Disturbance of endoplasmic reticulum proteostasis in neurodegenerative diseases. *Nature Reviews Neuroscience*, 15(4):233–249, April 2014.

[19] Claudio Hetz, Milene Russelakis-Carneiro, Kinsey Maundrell, Joaquin Castilla, and Claudio Soto. Caspase-12 and endoplasmic reticulum stress mediate neurotoxicity of pathological prion protein. *The EMBO Journal*, 22(20):5435–5445, October 2003.

[20] Claudio Hetz and Smita Saxena. ER stress and the unfolded protein response in neurodegeneration. *Nature Reviews Neurology*, 13(8):477–491, August 2017.

[21] Claudio Hetz, Kezhong Zhang, and Randal J. Kaufman. Mechanisms, regulation and functions of the unfolded protein response. *Nature Reviews Molecular Cell Biology*, 21(8):421–438, August 2020.

[22] Yang Kuang. *Delay differential equations: with applications in population dynamics*. Mathematics in science and engineering. Elsevier, Burlington, MA, 1993.

[23] Paul Lemarre, Laurent Pujo-Menjouet, and Suzanne S. Sindi. Generalizing a mathematical model of prion aggregation allows strain coexistence and co-stability by including a novel misfolded species. *Journal of Mathematical Biology*, 78(1):465–495, January 2019.

[24] Joanna Masel, Vincent A.A. Jansen, and Martin A. Nowak. Quantifying the kinetic parameters of prion replication. *Biophysical Chemistry*, 77(2):139–152, March 1999.

[25] Franziska Matthäus. Diffusion versus network models as descriptions for the spread of prion diseases in the brain. *Journal of Theoretical Biology*, 240(1):104–113, May 2006.

[26] Julie A. Moreno, Mark Halliday, Colin Molloy, Helois Radford, Nicholas Verity, Jeffrey M. Axten, Catharine A. Ortori, Anne E. Willis, Peter M. Fischer, David A. Barrett, and Giovanna R. Mallucci. Oral Treatment Targeting the Unfolded Protein Response Prevents Neurodegeneration and Clinical Disease in Prion-Infected Mice. *Science Translational Medicine*, 5(206):206ra138, October 2013.

[27] Julie A. Moreno, Helois Radford, Diego Peretti, Joern R. Steinert, Nicholas Verity, Maria Guerra Martin, Mark Halliday, Jason Morgan, David Dinsdale, Catherine A. Ortori, David A. Barrett, Pavel Tsaytler, Anne Bertolotti, Anne E. Willis, Martin Bushell, and Giovanna R. Mallucci. Sustained translational repression by eIF2α-P mediates prion neurodegeneration. *Nature*, 485(7399):507–511, May 2012.

[28] Stanley B. Prusiner. Prions. *Proceedings of the National Academy of Sciences*, 95(23):13363–13383, 1998.

[29] Stanley B Prusiner, Michael R Scott, Stephen J DeArmond, and Fred E Cohen. Prion Protein Biology. *Cell*, 93(3):337–348, May 1998.

[30] Jan Prüss, Laurent Pujo-Menjouet, Glenn F Webb, and Rico Zacher. Analysis of a model for the dynamics of prions. *Discrete & Continuous Dynamical Systems-B*, 6(1):225, 2006.

[31] Thorsten Pöschel, Nikolai V. Brilliantov, and Cornelius Frömmel. Kinetics of Prion Growth. *Biophysical Journal*, 85(6):3460–3474, December 2003.

[32] Xavier Roucou and Andréa C. LeBlanc. Cellular prion protein neuroprotective function: implications in prion diseases. *Journal of Molecular Medicine*, 83(1):3–11, January 2005.

[33] Benoit Schneider, Anne Baudry, Mathéa Pietri, Aurélie Alleaume-Butaux, Chloé Bizingre, Pierre Nioche, Odile Kellermann, and Jean-Marie Launay. The Cellular Prion Protein—ROCK Connection: Contribution to Neuronal Homeostasis and Neurodegenerative Diseases. *Frontiers in Cellular Neuroscience*, 15:101, 2021.

[34] S. Schnell. A Model of the Unfolded Protein Response: Pancreatic β-Cell as a Case Study. *Cellular Physiology and Biochemistry*, 23(4-6):233–244, 2009.

[35] L. F. Shampine and S. Thompson. Solving DDEs in Matlab. *Applied Numerical Mathematics*, 37(4):441–458, June 2001.

[36] Suzanne S. Sindi. Mathematical Modeling of Prion Disease. In Yusuf Tutar, editor, *Prion - An Overview*, page Ch. 10. IntechOpen, Rijeka, 2017.

[37] Hal Smith. *An Introduction to Delay Differential Equations with Applications to the Life Sciences*. Springer, New York, 2011.

[38] Heather L. Smith, Oliver J. Freeman, Adrian J. Butcher, Staffan Holmqvist, Ibrahim Humoud, Tobias Schätzl, Daniel T. Hughes, Nicholas C. Verity, Dean P. Swinden, Joseph Hayes, Lis de Weerd, David H. Rowitch, Robin J.M. Franklin, and Giovanna R. Mallucci. Astrocyte Unfolded Protein Response Induces a Specific Reactivity State that Causes Non-Cell-Autonomous Neuronal Degeneration. *Neuron*, 105(5):855–866.e5, March 2020.

[39] Heather L. Smith and Giovanna R. Mallucci. The unfolded protein response: mechanisms and therapy of neurodegeneration. *Brain*, 139(8):2113–2121, August 2016.

[40] Claudio Soto. Unfolding the role of protein misfolding in neurodegenerative diseases. *Nature Reviews Neuroscience*, 4(1):49–60, January 2003.

[41] Claudio Soto and Sandra Pritzkow. Protein misfolding, aggregation, and conformational strains in neurodegenerative diseases. *Nature Neuroscience*, 21(10):1332–1340, October 2018.

[42] M P Stumpf and D C Krakauer. Mapping the parameters of prion-induced neuropathology. *Proc Natl Acad Sci U S A*, 97(19):10573–10577, September 2000.

[43] Misaki Tanaka, Takeshi Yamasaki, Rie Hasebe, Akio Suzuki, and Motohiro Horiuchi. Enhanced phosphorylation of PERK in primary cultured neurons as an autonomous neuronal response to prion infection. *PLOS ONE*, 15(6):e0234147, June 2020.

[44] Joan Torrent, Davy Martin, Angélique Igel-Egalon, Vincent Béringue, and Human Rezaei. High-Pressure Response of Amyloid Folds. *Viruses*, 11(3), 2019.

[45] Mauricio Torres, Karen Castillo, Ricardo Armisén, Andrés Stutzin, Claudio Soto, and Claudio Hetz. Prion Protein Misfolding Affects Calcium Homeostasis and Sensitizes Cells to Endoplasmic Reticulum Stress. *PLOS ONE*, 5(12):e15658, December 2011.

[46] A. Trusina and C. Tang. The unfolded protein response and translation attenuation: a modelling approach. *Diabetes, Obesity and Metabolism*, 12(s2):27–31, October 2010.

[47] Ala Trusina, Feroz R. Papa, and Chao Tang. Rationalizing translation attenuation in the network architecture of the unfolded protein response. *Proc Natl Acad Sci USA*, 105(51):20280, December 2008.

[48] Johannes Weickenmeier, Ellen Kuhl, and Alain Goriely. Multiphysics of Prionlike Diseases: Progression and Atrophy. *Phys. Rev. Lett.*, 121(15):158101, October 2018.

[49] R. Luke Wiseman, Evan T. Powers, Joel N. Buxbaum, Jeffery W. Kelly, and William E. Balch. An Adaptable Standard for Protein Export from the Endoplasmic Reticulum. *Cell*, 131(4):809–821, November 2007.